Mineralium Deposita (2002) 37: 568–586
DOI 10.1007/s00126-002-0274-7

ARTICLE

Alain Dupont · Jacqueline Vander Auwera
Christian Pin · Ştefan Marincea · Tudor Berza

Trace element and isotope (Sr, Nd) geochemistry of porphyry- and skarn-mineralising Late Cretaceous intrusions from Banat, western South Carpathians, Romania

Received: 28 December 2001 / Accepted: 11 January 2002 / Published online: 1 May 2002

Abstract Geochemical and isotopic (strontium, neodymium) data have been obtained from 24 samples of seven Late Cretaceous intrusions associated with skarn (Tincova, Bocşa, Ocna de Fier – Dognecea) and porphyry copper-molybdenum/skarn deposits (Oraviţa, Ciclova, Sasca and Moldova Nouă) in the South Carpathians of Romania. The intrusions cut the Supragetic-Getic nappes and form a 100-km-long, NNE-SSW-trending lineament in the Banat metallogenic province. The samples range in composition from gabbro to granodiorite and define, in major and trace element variation diagrams, a calc-alkaline to high-potassium calc-alkaline trend ranging from 50 to 67% SiO_2. They are magnetite-bearing, I-type granitoids enriched in LILE/LREE and depleted in Nb, Ta and Zr, common features for magmas associated with subduction zones. The lack of cumulate textures and of positive europium anomalies seems to indicate that the samples represent liquid compositions. The observed trend thus approximates a liquid line of descent resulting from fractional crystallisation of parental magmas with similar major and trace element compositions. Initial strontium isotopic ratios (Sr_i) vary from 0.7042 to 0.7058 and $\epsilon_{Nd(t)}$ values range from +3.9 to –0.2. Variations of Sr_i and $\epsilon_{Nd(t)}$ values with SiO_2 show minor crustal assimilation. The generally positive $\epsilon_{Nd(t)}$ values, together with moderate Sr_i, indicate that the parental magmas result from partial melting of a rubidium-enriched and LREE-depleted source, such as a heterogeneous lithospheric mantle or a young mafic lower crust derived from it. Selective rubidium enrichment probably occurred during a previous subduction event by metasomatism of the overlying mantle wedge, either in the Early Cretaceous or earlier, as suggested by T_{DM} model ages (ca. 600 Ma). The Cu-Mo(-Pb-Zn-Fe) deposits are intimately associated with the intrusions, and the Banat (Romania) region can be subdivided in two metallogenic zones. In northern Banat, Fe-Cu-Pb-Zn skarns occur whereas in southern Banat, porphyry-style copper and molybdenum deposits predominate. These differences result from a combination of several parameters: (1) magma composition, whereby copper- and molybdenum-rich deposits tend to be associated with calc-alkaline compositions; (2) an increase of the present-day erosion level, from south to north, as indicated by the presence of large equigranular plutons in northern Banat, and of porphyritic cupolas and apophyses associated with porphyry-style mineralisation in southern Banat; (3) the nature of the host rocks, with skarns preferentially developed in calcareous host rocks; and (4) local variations of conditions controlling the infiltration of fluids and the precipitation of ore minerals.

Keywords Banat · Late Cretaceous · Geochemistry · Fractional crystallisation · Mineralisation

A. Dupont (✉) · J. Vander Auwera
L.A. Géologie, Pétrologie et Géochimie,
Bâtiment B20, Université de Liège,
4000 Liège, Belgium
E-mail: a.dupont@student.ulg.ac.be
Tel.: +32-43662257
Fax: +32-43662921

C. Pin
Laboratoire Magmas et Volcans,
U.M.R. 6524 CNRS, Unité de Géochimie,
Université Blaise Pascal, 5 rue Kessler,
63038 Clermont-Ferrand Cedex, France

Ş. Marincea · T. Berza
Geological Institute of Romania,
Caransebeş Str. 1, Bucharest 78344, Romania

Introduction

World-class ore deposits are associated with a belt of Late Cretaceous intrusions and volcano-plutonic complexes in western Romania (Apuseni and Banat Mountains), eastern Serbia (Ridanj-Krepoljin and Timok) and northern Bulgaria (Srednogorie). These igneous bodies form a discontinuous, elongated (50–100×1,500 km) belt called the Banatitic Magmatic and Metallogenetic Belt (BMMB) by Berza et al. (1998; Fig. 1, inset). Three

trends of evolution have previously been recognised within this belt (Berza et al. 1998): a monzodioritic/dioritic to granodioritic/granitic trend (South Apuseni, southern Banat, Timok, western and central Srednogorie), a granodioritic to granitic trend (North Apuseni, northern Banat, Ridanj-Krepoljin), and an alkaline trend with considerable petrographic variability (western part of northern Banat, eastern and western Srednogorie).

Although numerous studies have been carried out on the ore deposits associated with these intrusions (e.g. von Cotta 1864; Codarcea 1931; Cioflica and Vlad 1973; Russo-Săndulescu and Berza 1979; Vlad 1979, 1997; Vassiliev and Stanisheva-Vassilieva 1981; Popov 1981, 1996; Cioflica 1989; Jankovic 1997; Karamata et al. 1997a; Nicolescu and Cornell 1999), most geochemical data to date for the host plutons were obtained solely by wet chemical analyses (e.g. Divljan and Karamata 1967; Drovenik et al. 1967; Boccaletti et al. 1978; Russo-Săndulescu et al. 1978, 1986a, 1986b; Russo-Săndulescu and Berza 1979; Constantinescu 1980; Popov 1981; Djordjevic et al. 1997). Few trace element and isotopic data, obtained by more modern and precise techniques, are available (Ştefan et al. 1992; Cioflica et al. 1996, 1997; Nicolescu et al. 1999). Ştefan et al. (1992) presented XRF (Rb, Sr, Y, Zr and Nb) and INAA (La, Ce, Sm, Eu, Tb, Hf and Th) analyses for intrusions cropping out in the northern Apuseni Mountains (Romania). Cioflica et al. (1996, 1997) and Nicolescu et al. (1999) focused on the Banat Mountains (Romania). Nicolescu et al. (1999) reported secondary ion mass spectrometry (SIMS) U-Pb zircon ages for the Bocşa and Ocna de Fier – Dognecea intrusions, together with two trace element analyses by ICP-MS. Cioflica et al. (1996, 1997) mostly studied intrusions from southern Banat, discussing their origin on the basis of unpublished chemical analyses and some isotopic data ($^{87}Sr/^{86}Sr = 0.70527–0.70587$ and $^{143}Nd/^{144}Nd = 0.51255–0.51275$). This lack of comprehensive geochemical and isotopic data led us to undertake the following work.

We report data for seven ore-related Late Cretaceous intrusions that cut the Middle Cretaceous Supragetic-Getic nappes (Iancu 1986), which form the western part of the South Carpathians (Banat Mountains, Romania): Moldova Nouă, Sasca, Ciclova, Oraviţa, Ocna de Fier – Dognecea, Bocşa (units 1 to 3, Russo-Săndulescu and Berza 1979) and Tincova (Fig. 1). The intrusions are mafic to felsic in composition, and are commonly referred to as 'banatites' following the work of von Cotta (1864).

The spatial distribution of skarn and porphyry deposits follows a N-S-orientated lineament defined by intrusions emplaced along a zone of weakness. Because magmatism and hydrothermal ore formation occurred along the same structures, by inference, they are related to a common process (Cioflica and Vlad 1973). There also seems to be a metal zonation throughout the Banat region (Vlad 1997), with a transition from copper- and molybdenum-rich deposits in the south, through molybdenum-rich ores in the centre, to iron-, lead- and zinc-rich systems in the north. Vlad (1979, 1997) related this metallogenic zonation to a subduction zone dipping towards the north-west. In southern Banat, porphyry copper-molybdenum deposits and related skarns occur at Moldova Nouă whereas at Sasca, only copper (-molybdenum) skarn deposits are found. Porphyry copper (-molybdenum) deposits are also present at Ciclova. A subeconomic stockwork mineralisation is associated with the Oraviţa intrusion. Copper (-molybdenum) skarn deposits, linked to these two intrusions, have also been discovered. In northern Banat, only skarn deposits occur. The more important are the skarn deposits of the Ocna de Fier – Dognecea district (e.g. von Cotta 1864; Codarcea 1931; Vlad 1974; Nicolescu and Cornell 1999; Nicolescu et al. 1999) which can be divided into a proximal iron- and copper-rich part and a distal lead- and zinc-dominated part. The Bocşa intrusion lacks economic mineralisation, but Fe-Pb-Zn(-Cu) skarn deposits are associated with the Tincova intrusion (Table 1).

The aim of the present work was to obtain geochemical (major and trace elements) and isotopic (strontium and neodymium) data on the above-mentioned intrusions to characterise their geochemical signatures and their possible parental magma sources. These data will be used to check whether or not the metallogenic zonation observed by Vlad (1979, 1997) can be related to different magmatic evolution trends, as recently suggested by Berza et al. (1998).

Geological setting

The Carpathians are part of the European Alpine system and form a mountainous belt which continues westwards to the Alps and eastwards to the Balkans. The European Alpine system results from the Cretaceous-Tertiary convergence and collision between the European and Apulian (African) plates, which caused the closure of the Tethys and other oceans (Burchfiel 1980). The Carpathian Fold and Thrust Belt is represented by several mountain ridges: the West Carpathians, the Apuseni Mountains (central outcrop), the East Carpathians and the South Carpathians, with the latter being curved from E–W to N–S. When considered together with the Balkan Mountains (and Srednogorie region) in Bulgaria, the South Carpathians constitute a horseshoe-like physiographic feature partly surrounding the Moesian platform (Fig. 1, inset). This shape was interpreted as resulting from a 'corner effect' induced by the Moesian platform during Alpine collision in the Tertiary, causing rotation, wrenching and a lateral translation of the Cretaceous nappe pile (Ratschbacher et al. 1993; Schmid et al. 1998).

The foreland of the South Carpathians is the Moesian platform, a Late Proterozoic basement block covered by thick Paleozoic and Mesozoic sedimentary rock sequences (Săndulescu 1994). The Carpathian nappe pile was thrust during the Miocene onto the flat Moesian

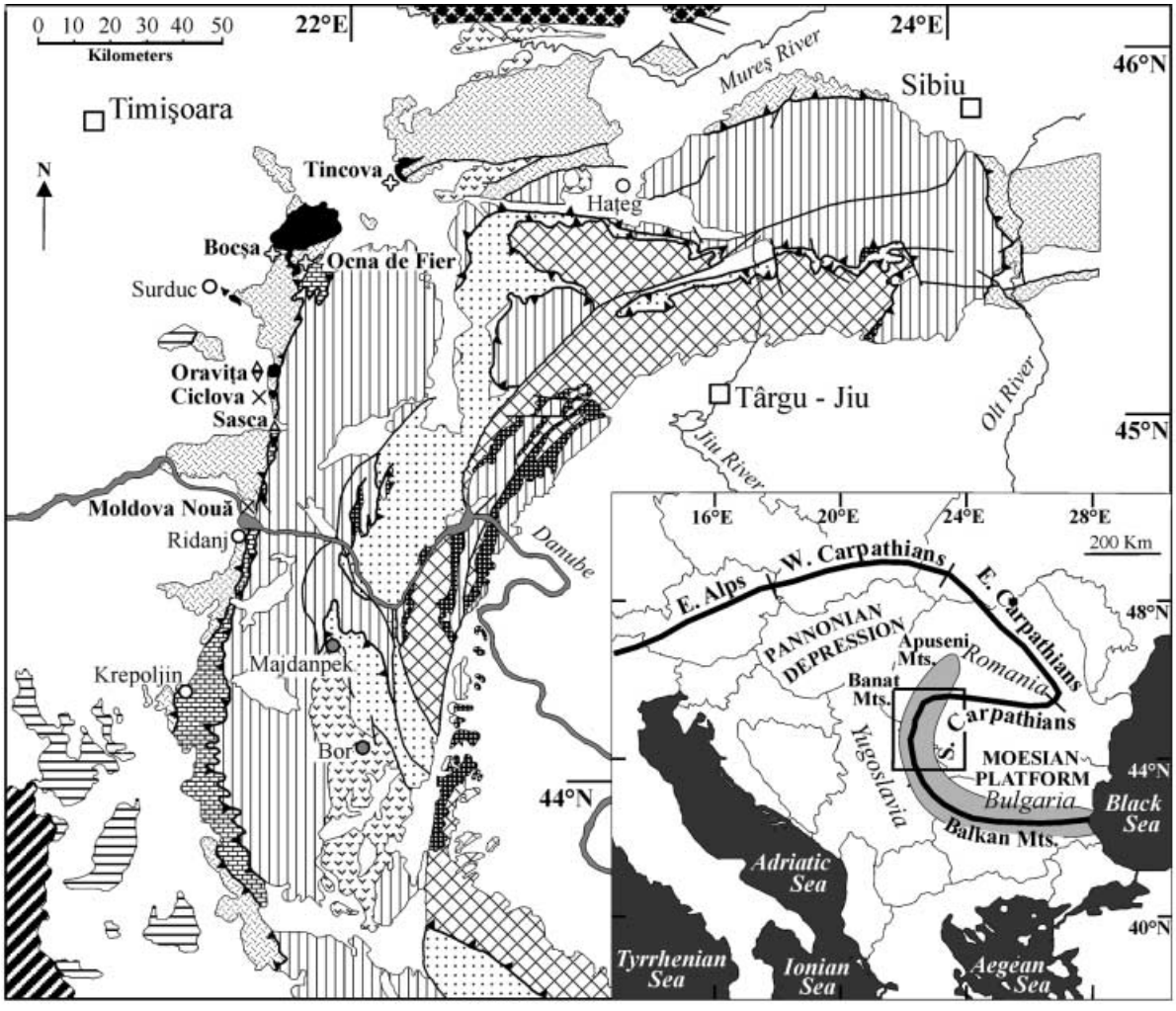

Post-tectonic covers and magmatites
- Tertiary - Quaternary sediments
- Upper Cretaceous intrusions
- Upper Cretaceous volcanics

Vardar - Transylvanian Terrane
- Vardar units
- Transylvanian nappes

Bucovino - Getic Terrane
- Serbo - Macedonian Nappe
- Supragetic Nappe
- Sasca - Gornjak Nappe
- Getic Nappe

Civcin - Ceahlău - Severin Terrane
- Severin Nappe

Danubian Terrane
- Upper Danubian Nappe
- Lower Danubian Nappe

Inset
- Alps - Balkan Mts. - Carpathians orogenic chain
- BMMB

Symbols
- Fault
- Thrust fault
- Town
- Village
- Fe-Pb-Zn skarn deposits
- Mo skarn deposit
- Cu (Mo) skarn deposit
- Cu (Mo) porphyry and skarn deposits
- Cu (Au-Mo) (major) porphyry deposits + skarn deposits and massive sulfides

◄

Fig. 1 Geological sketch map of the western South Carpathians (modified after Kräutner 1997), showing the main units and nappes, the studied calc-alkaline intrusions (*bold letters*) and the associated ore deposits (refer to Table 2 for a brief description of these units and nappes). Smaller intrusions are slightly enlarged. *Inset* shows south-eastern Europe with the axis of the mainly Tertiary Alps – Carpathian – Balkans orogenic chain, and the axis of the Late Cretaceous Banatitic Magmatic and Metallogenetic Belt (BMMB)

cover (Ştefănescu 1988). The internal part of the Carpathian orogen is represented by the Fore-Apulian continental blocks of the northern Apuseni Mountains, and by most of the pre-Tertiary basement beneath the north-eastern part of the Pannonian Depression. The Fore-Apulian domain is bordered seawards by Triassic to Jurassic ophiolitic and flysch belts (Vardar to the south, Transylvanian to the east, Pieniny to the north), which are considered to mark the main Tethyan suture (Săndulescu and Visarion 2000). In the East and South Carpathians, these ophiolitic belts are bordered by units representing the European continental margin. A separate ocean (Ceahlău-Severin) formed in the Late Jurassic and closed in the Middle Cretaceous (Săndulescu 1994).

The South Carpathians are made up of three nappes systems, defined from top to bottom (Fig. 1, Table 2) as the Supragetic-Getic nappes, the Severin Nappe, and the Danubian nappes (Berza 1997). The Supragetic-Getic nappes consist of Variscan basement units with an Upper Carboniferous to Lower Cretaceous cover, imbricated during Middle Cretaceous stacking (Iancu 1985, 1986). Both the Supragetic-Getic nappe pile and overlying Late Cretaceous basins, which are filled by synorogenic clastic sediments (Gosau-type basins; Willingshofer 2000) are intruded by Late Cretaceous plutons and some of these basins contain volcanic rocks. The intermediate Severin Nappe consists of slices of the Severin palaeo-ocean floor (ophiolites) covered by Late Jurassic-Early Cretaceous flysch formations. Together with the Supragetic-Getic nappe pile, the Severin Nappe was thrust in the latest Cretaceous onto the Danubian nappes and is now exposed as an oceanic unit between two continental units. The Danubian nappes consist of latest Proterozoic (Pan-African) basement rocks (Liégeois et al. 1996) overlain by Silurian-Permian and Jurassic-Upper Cretaceous cover formations, mainly metamorphosed to low grades. The stacking of the Danubian nappes did not occur before the Late Cretaceous because Senonian flysch is preserved at their top. In the Senonian flysch from the Lainici Lower Danubian Nappe, metre-thick beds of andesitic tuffs of unknown origin can be observed (Savu et al. 1987). In the western part of the South Carpathians (Supragetic-Getic domain, Bucovino-Getic terrane), Late Cretaceous magmas erupted in the Gosau-type Rusca Montană and Haţeg basins, whereas in the Banat Mountains, only major plutons or dyke swarms cut the pre-Alpine basement and/or the Mesozoic cover. These intrusions are the focus of our study.

Most studies relate the Late Cretaceous magmatism to Early Cretaceous subduction of various palaeo-oceans, either westwards (Rădulescu and Săndulescu 1973; Russo-Săndulescu et al. 1978; Vlad 1979; Russo-Săndulescu et al. 1986a, 1986b; Cioflica et al. 1996; Vlad 1997) or eastwards (Boccaletti et al. 1974; Vassiliev and Stanisheva-Vassilieva 1981; Jankovic 1997; Karamata et al. 1997a). Boccaletti et al. (1974) considered that the closure of the Vardar Ocean occurred in the Middle Cretaceous and suggested that magmas resulted from Late Cretaceous slab detachment. By contrast, Nicolescu et al. (1999) advocated a post-collisional setting for the emplacement of the Ocna de Fier – Dognecea and Bocşa 3 intrusions, on the basis of precise age determinations and the fact that the Late Cretaceous plutons cut the Middle Cretaceous faults bordering the Supragetic units. Some authors also relate the Late Cretaceous magmatism in the Carpathians and Balkans to extensional domains, such as rift valleys, grabens and normal faults (Grubić 1974; Popov 1981, 1987, 1996; Berza 1999). The presence of extensional basins in the South

Table 1 Relation between the position of the studied intrusions (Banat, Romania), their emplacement conditions and the associated ore deposits. Metals mentioned between parentheses occur in lesser abundance

Area	Intrusion	Emplacement conditions	Type(s) of ore deposits	Metals[a]	Status
North Banat	Tincova	Plutonic	Skarn deposits	Fe, Pb, Cu, Zn (Mo)	Prospect
	Bocşa			Pb, Zn (Bocşa 3)	Occurrence
	Ocna de Fier-Dognecea			Fe, (Cu): proximal skarn Pb, Zn: distal skarn	Mined in the past
South Banat	Oraviţa	Plutonic to subvolcanic	Minor porphyry-mineralisations and skarn deposits	Mo, (W, Au, Cu, Pb, Zn)	Mined in the past, Au prospect[b]
	Ciclova		Porphyry and skarn deposits	Cu (Mo, W, Co, Au)	Mined in the past, Au prospect[b]
	Sasca		Skarn deposits	Cu (Mo)	Mined in the past
	Moldova Nouă		Porphyry and skarn deposits	Cu (Mo)	In activity (Suvarov open-pit)

[a]Karamata et al. (1997a), Vlad (1997)
[b]Ciobanu (personal communication)

Table 2 Brief description of the units (or nappe/nappes) which make up the South Carpathians. All the descriptions are based on Berza (1997), except the ones relative to the Vardar and Serbo-Macedonian units which are based on Arsovski and Dumužanov (1995) and Karamata et al. (1997b)

Terrane	Nappe/nappes or units	Description
Vardar-Transylvanian terrane	Vardar units	Triassic sandstones, rhyolites, spilites and limestones; Jurassic ophiolites, granites, turbidites and limestones; Lower Cretaceous laterites; Upper Cretaceous wildflysch; Eocene flysch
	Transylvanian nappes	Lower-Middle Jurassic ophiolites and island-arc magmatites; Upper Jurassic limestones; Lower Cretaceous flysch; Upper Cretaceous wildflysch
Bucovino-Getic terrane	Serbo-Macedonian nappes	Upper Proterozoic metamorphic basement; Lower Paleozoic metabasic and metadetrital formations; Upper Carboniferous-Permian detritals; Upper Cretaceous flysch
	Supragetic nappes	Upper Proterozoic metamorphic basement; Upper Devonian-Lower Carboniferous metabasic and metadetrital formations; Upper Carboniferous and Middle Jurassic detritals; Upper Jurassic sandstones and limestones; Lower Cretaceous limestones; Upper Cretaceous marls
	Sasca-Gornjak Nappe	Upper Carboniferous conglomerates; Permian sandstones; Lower-Middle Triassic conglomerates and limestones; Lower Jurassic detritals; Middle Jurassic marls; Upper Jurassic limestones
	Getic nappes	Upper Proterozoic metamorphic-granitic basement; Lower Paleozoic metabasic and metadetrital formations; Upper Carboniferous coal-bearing detritals; Permian-Lower Jurassic detritals; Middle Jurassic marls; Upper Jurassic limestones; Lower Cretaceous marls and limestones; Upper Cretaceous Gosau-type detritals
Civcin-Ceahlău-Severin terrane	Severin Nappe	Upper Jurassic-Lower Cretaceous turbidites and ophiolites
Danubian terrane	Upper Danubian nappes	Upper Proterozoic metamorphic-granitic basement; Ordovician-Devonian detritals and rhyolites; Lower Carboniferous limestones; Upper Carboniferous coal-bearing detritals; Permian detritals and rhyolites; Jurassic detritals and limestones; Lower Cretaceous marls and limestones; Upper Cretaceous flysch
	Lower Danubian nappes	Upper Proterozoic metamorphic-granitic basement; Ordovician-Devonian and Permian detritals and rhyolites; Lower Jurassic detritals; Middle Jurassic-Lower Cretaceous limestones; Upper Cretaceous flysch

Carpathians is not in conflict with geochemical evidence for a subduction-related magmatism. The studied intrusions were emplaced concomitantly with others located in such basins, and we consider that a Vardar slab detachment process ('slab breakoff', von Blanckenburg and Davies 1995) triggered the rising of the parental magmas.

Petrography

Because of poor outcrop in the wooded western South Carpathians, this study was focused on the mineralisation-related intrusions, where fresh samples could be collected (old mines or valley outcrops). We avoided zones of hydrothermal alteration and only fresh samples were analysed. The exact co-ordinates of our sampling sites are given in Table 3, and more precise locations are plotted on scanned geological map segments which can be obtained from the corresponding author upon request. Table 4 summarises our petrographic descriptions of the samples.

Plotted in the P-Q diagram of Debon and Lefort (1983; Fig. 2), samples range from gabbroic to granodioritic compositions, with intermediate compositions being the most abundant. Most samples are coarse-grained with a heterogranular to porphyritic (plagioclase, biotite and amphibole phenocrysts) texture. Rounded, mafic, microgranular enclaves (MME) present in some of the most felsic samples are more altered (biotite and hornblende chloritisation, feldspar saussuritisation) than the host rock and contain host phenocrysts. Plagioclase, K-feldspar, quartz, biotite and hornblende are major phases occurring in variable proportions. Apatite, titanite and opaque minerals are ubiquitous accessory phases. Zircon, clinopyroxene, orthopyroxene and allanite are sporadically observed. Clinopyroxene mostly occurs as relics in hornblende crystals. Within Bocşa 1 and 2 intrusions, orthopyroxene consists of hypersthene, whereas clinopyroxene is an augite with pigeonite exsolutions (Russo-Săndulescu et al. 1978). The anorthite content of plagioclase was optically determined (An_{30} to An_{70}). Plagioclase is hypidiomorphic and usually displays recurrent zoning.

Table 3 Location of the studied samples from Banat (Romania)

Intrusion	Outcrop	Sample	Co-ordinates	
			Latitude (N)	Longitude (E)
Tincova	9-km NE–SW length and a maximum 4-km width[a]	98R18	45°37′50″	22°14′02″
		98R20	45°37′42″	22°14′56″
		98R22	45°30′20″	22°15′11″
		98R23	45°30′21″	22°15′12″
Bocşa 1	25-km NE–SW length and a maximum 15-km for the whole Bocşa intrusion (3 units)[b]	95R13	45°26′08″	21°44′59″
		95R15	45°25′08″	21°44′57″
		98R02	45°28′15″	21°45′02″
Bocşa 2		95R07	45°25′43″	21°45′10″
		95R09	45°25′45″	21°45′08″
		95R11	45°25′47″	21°45′05″
Bocşa 3		98R13	45°26′48″	21°45′15″
		98R16	45°27′30″	21°45′14″
Ocna de Fier-Dognecea	15-km N–S length and a maximum 5-km width[c]	98R04	45°19′07″	21°45′42″
Oraviţa	These intrusions from South Banat consist of outcrops of several km^2 belonging to a 60-km-long and 5-km-wide N–S-trending belt	95R04	45°04′25″	21°44′25″
		98R05	45°04′27″	21°43′14″
		98R07	45°04′25″	21°43′12″
		98R08	45°04′24″	21°43′11″
		98R09	45°02′58″	21°44′14″
		98R10	45°02′54″	21°44′06″
Ciclova		98R11	45°01′48″	21°44′32″
		98R12	45°01′49″	21°44′42″
Sasca		98R24	44°50′48″	21°45′07″
		98R26	44°52′18″	21°45′06″
Moldova Nouă		98R27	44°46′41″	21°44′58″

[a]Andrei et al. (1988)
[b]Berza (personal communication)
[c]Russo-Săndulescu et al. (1986b)

Its habit suggests early crystallisation, and a slight orientation (magmatic lamination) is locally observed. Potassium feldspar is often perthitic and corresponds to intermediate microcline in the Bocşa intrusion (Russo-Săndulescu et al. 1978). Its interstitial structure, a feature that it shares with quartz, points to a late crystallisation. Hornblende and biotite (± opaque minerals) often agglomerate and form schlieren textures. Hornblende crystallised after plagioclase and was closely followed by biotite. The opaque minerals of Bocşa mainly consist of titano-magnetite with ilmenite exsolutions, magnetite, pyrite and chalcopyrite (Russo-Săndulescu et al. 1978).

All samples contain hornblende, biotite, titanite and magnetite. These are the well-recognised, characteristic minerals for I-type (Chappell and White 1974) and magnetite-series granitoids (Ishihara 1977).

Analytical methods

Major and trace elements

Major and trace elements analyses (Table 5) were performed at the Laboratoires Associés de Géologie, Pétrologie et Géochimie of the Université de Liège (Belgium). Concentrations were measured by X-ray fluorescence (XRF) spectrometry following Bologne and Duchesne (1991), with an Alpha 2020 CGR instrument and using lithium borate (enriched in La_2O_3) glass discs for major elements (except Na_2O) and pressed powder pellets for Na_2O, Rb, Sr, Zr, Nb, Y, Zn, Ni and Cr. Other trace element concentrations were obtained by the ICP-MS technique of Vander Auwera et al. (1998b), using a VG Elemental Plasma Quad PQ2 spectrometer, except for samarium and neodymium which were determined by isotope dilution.

Strontium and neodymium isotope data

Isotope analyses were performed at the Université Blaise Pascal de Clermont-Ferrand (France) on an upgraded VG 54E thermal ionisation mass spectrometer (TIMS). The procedure largely followed that of Pin and Bassin (1992) and Pin and Santos Zalduegui (1997). Samarium and neodymium concentrations were obtained by isotope dilution using a mixed ^{149}Sm-^{150}Nd-enriched tracer. The mass spectrometer was used in triple-collection mode for strontium and neodymium, and in single-collection mode for samarium. Strontium mass fractionation was corrected by normalising to $^{86}Sr/^{88}Sr = 0.1194$ (Steiger and Jäger 1977), and neodymium mass fractionation was corrected by normalising to

Table 4 Petrography of the samples coming from the studied intrusions (Banat, Romania). *all* Allanite, *ap* apatite, *bio* biotite, *cpx* clinopyroxene, *horn* hornblende, *ksp* K-feldspar, *op* opaques, *opx* orthopyroxene, *pl* plagioclase, *qz* quartz, *tit* titanite, *zir* zircon

Intrusion	Sample	Rock type[a]	Major phases	Accessories	Structure	Remarks
Tincova	98R18	Quartz monzodiorite	Bio, horn, pl, ksp, qz	Op, ap, tit, zir	Heterogranular	Poecilitic K-feldspar
	98R20	Granodiorite	Bio, horn, pl, ksp, qz	Op, ap, tit, zir, all	Hypidiomorph heterogranular	
	98R22	Quartz monzodiorite	Bio, horn, pl, qz	Op, ap, tit	Porphyric	
	98R23	Granodiorite	Bio, horn, pl, ksp, qz	Op, ap, tit, zir	Hypidiomorph	Quartz monzodiorite enclave present
Bocşa 1	95R13	Quartz monzodiorite	Bio, horn, pl, ksp, qz	Op, ap, tit	Heterogranular	
	95R15	Gabbro	Bio, cpx, pl, ksp	Op, ap, tit	Heterogranular	Poecilitic K-feldspar
	98R02	Monzodiorite	Bio, horn, pl, ksp, qz	Op, ap, tit, cpx	Heterogranular	Poecilitic K-feldspar
Bocşa 2	95R07	Tonalite	Bio, horn, pl, ksp, qz	Op, ap, tit, zir	Hypidiomorph granular	Opaques symplectites within plagioclase
	95R09	Quartz monzodiorite	Bio, horn, pl, ksp, qz	Op, ap, tit	Hypidiomorph granular	
	95R11	Quartz monzodiorite	Bio, horn, pl, ksp, qz	Op, ap, tit	Heterogranular	Opaques symplectites within plagioclase
Bocşa 3	98R13	Quartz monzodiorite	bio, horn, pl, ksp, qz	Op, ap, tit, zir	Heterogranular	
	98R16	Granodiorite	Bio, horn, pl, ksp, qz	Op, ap, tit, zir	Hypidiomorph heterogranular	Poecilitic K-feldspar
Ocna de Fier-Dognecea	98R04	Granodiorite	Bio, horn, pl, ksp, qz	Op, ap, tit	Heterogranular	Poecilitic biotite and K-feldspar
Oraviţa	95R04	Granodiorite	Bio, horn, pl, ksp, qz	Op, ap, tit, zir	Porphyric	Poecilitic biotite
	98R05	Quartz diorite	Bio, horn, pl, ksp, qz	Op, ap, tit	Porphyric	Mafic microgranular enclave (MME)
	98R07	Granodiorite	Bio, horn, pl, ksp, qz	Op, ap, tit	Heterogranular	Poecilitic biotite
	98R08	Granodiorite	Bio, horn, pl, ksp, qz	Op, ap, tit	Porphyric	Poecilitic biotite and K-feldspar
	98R09	Quartz monzodiorite	Bio, horn, pl, ksp, qz	Op, ap, tit, cpx	Heterogranular	Poecilitic K-feldspar
	98R10	Quartz diorite	Bio, horn, pl	Op, ap, tit	Heterogranular	Slight cumulate texture
Ciclova	98R11	Quartz diorite	Bio, horn, pl, ksp, qz	Op, ap, tit, opx	Hypidiomorph granular	Poecilitic K-feldspar
	98R12	Gabbro	Bio, horn, pl, ksp, qz	Op, ap, tit, cpx	Poecilitic	
Sasca	98R24	Quartz diorite	Bio, horn, pl, ksp, qz	Op, ap, tit, zir	Porphyric	
	98R26	Tonalite	Bio, horn, pl, ksp, qz	Op, ap, tit, zir	Heterogranular	
Moldova Nouă	98R27	Quartz diorite	Bio, horn, pl, ksp, qz	Op, ap, tit, zir	Heterogranular	

[a]Rock type obtained with Debon and Lefort (1983) nomenclature

$^{146}Nd/^{144}Nd = 0.7219$ (O'Nions et al. 1977). During this study, standard measurements gave an average $^{87}Sr/^{86}Sr$ of 0.710260 ± 12 ($2\ \sigma$) for seven runs of the NBS 987 standard, and average $^{143}Nd/^{144}Nd$ of 0.511958 ± 7 ($2\ \sigma$) and $^{145}Nd/^{144}Nd$ of 0.348413 ± 5 ($2\ \sigma$) for five runs of the AMES Rennes standard. An earlier intercalibration test had yielded an average $^{143}Nd/^{144}Nd$ of 0.511965 ± 12 ($2\ \sigma$) for ten runs of the AMES Rennes standard, and an average $^{143}Nd/^{144}Nd$ of 0.511851 ± 13 ($2\ \sigma$) for four runs of the La Jolla international standard.

Geochemistry

Typology

The TAS diagram (Fig. 3A) and the agpaïtic index (Liégeois and Black 1987, Fig. 3B), barely reaching 0.7 in the most felsic rocks, show the subalkaline nature of the samples. In an AFM diagram (Fig. 3C), the samples plot in the calc-alkaline field. This calc-alkaline character is corroborated by the Peacock index (Brown 1981, Fig. 3D). In a K_2O vs. SiO_2 diagram (Fig. 3E), the samples range in composition from calc-alkaline to high-potassium calc-alkaline, with sample 98R02 falling in the shoshonitic field. Samples do not show any A-type affinity in a Whalen et al. (1987) diagram (Fig. 3F). Geochemical data thus confirm that all granitoids have an I-type affinity.

Major and trace elements

Harker diagrams are presented in Fig. 4. Continuous depletion in $(Fe_2O_3)_t$, TiO_2, CaO and of the $CaO/(Na_2O + K_2O)$ ratio, with increasing SiO_2, confirms the early fractionation of Fe-Ti oxides and calcium-rich phases (clinopyroxene cores, hornblende, plagioclase, titanite). A continuous decrease of P_2O_5 with differentiation suggests that apatite is a liquidus phase, consistent with neodymium and samarium decrease. K_2O behaves incompatibly (Fig. 3E).

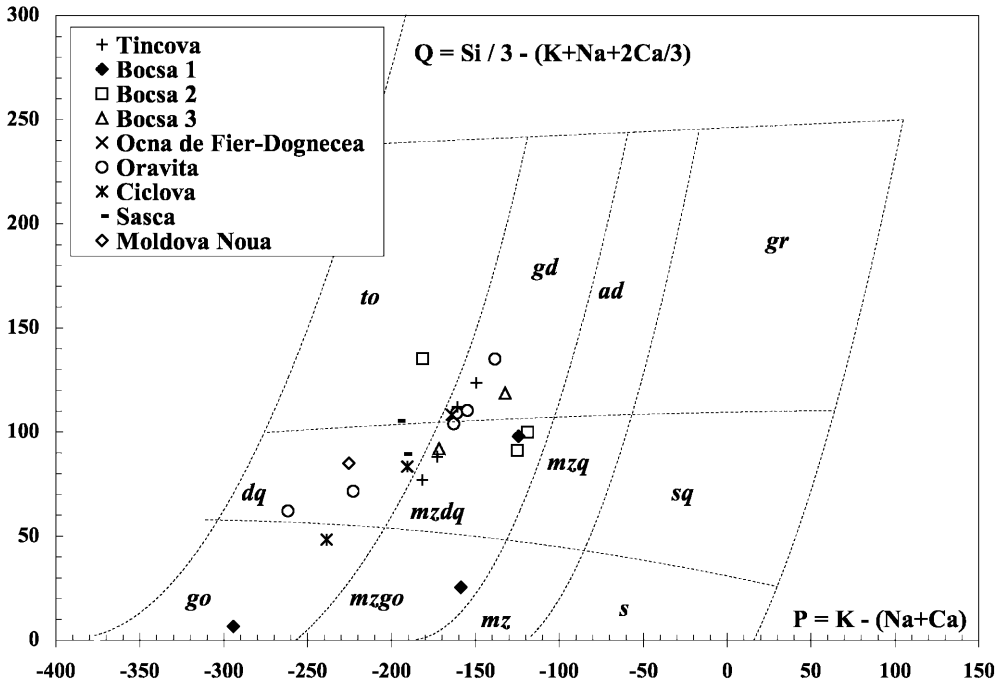

Fig. 2 Chemical classification of common igneous rocks of Debon and Lefort (1983). Parameters are expressed as gram-atoms$\times 10^3$ of each element in 100 g of rock. *go* Gabbro (diorite), *mzgo* monzogabbro (monzodiorite), *mz* monzonite, *s* syenite, *dq* quartz diorite (quartz gabbro), *mzdq* quartz monzodiorite (quartz monzogabbro), *mzq* quartz monzonite, *sq* quartz syenite, *to* tonalite, *gd* granodiorite, *ad* adamellite, *gr* granite

All samples fall into a restricted compositional range defined by the representative examples plotted in spidergrams of Fig. 5 and the chondrite-normalised rare earth elements (REE) patterns of Fig. 6. They display a clear enrichment in large ion lithophile elements (LILE) and a marked depletion in Nb, Ta and sometimes Zr (Fig. 5), typical of magmas associated with subduction zones. The samples are enriched in light REE (average $(La/Yb)_N = 14.2$) and usually display a slight negative europium anomaly ($Eu/Eu^* = 0.7$ to 0.9, Fig. 6). Variation diagrams (Fig. 4) show that the samples define a single trend even though they belong to seven distinct intrusions, and that they probably result from the crystallisation of magma batches of similar starting composition.

Strontium and neodymium isotopic data

Strontium and neodymium isotopic data are presented in Table 6. All measured isotopic ratios have been corrected for in situ decay assuming an age of 80 Ma based on the U-Pb zircon ages from Bocşa 3 (79.6 ± 2.5 Ma) and Ocna de Fier – Dognecea (75.5 ± 1.6 Ma; Nicolescu et al. 1999). These are the most reliable ages obtained so far for these intrusions, and they coincide with a Re-Os age on molybdenite from skarn mineralisation in the Ocna de Fier – Dognecea district (76.6 ± 0.3 Ma; Ciobanu et al. 2002, this volume). Even if the other intrusions were a few million years older or younger, as suggested by the available K-Ar ages (e.g. Russo-Săndulescu et al. 1986c; Soroiu et al. 1986; Strutinski et al. 1986), this would not result in significantly different initial isotopic compositions.

Initial strontium isotopic ratios (Sr_i) vary between 0.7042 and 0.7058, and $\epsilon_{Nd(t)}$ values range from +3.9 to –0.2, in agreement with data mentioned by Cioflica et al. (1996). In Sr_i versus SiO_2 and in $\epsilon_{Nd(t)}$ versus SiO_2 diagrams (Fig. 7A, C), data from the studied group of intrusions are scattered and no clear trend can be seen. Most samples cluster near $Sr_i = 0.705$ and $\epsilon_{Nd(t)} = 0$ to +2 (Fig. 7E). Six samples from the Oraviţa intrusion, when considered by themselves, display an increase of Sr_i and a decrease in $\epsilon_{Nd(t)}$ values with increasing SiO_2. A similar trend is apparent in two samples from Ciclova. Also, in the Oraviţa group, one sample (98R09) has the most juvenile isotopic composition ($Sr_i = 0.7043$ and $\epsilon_{Nd(t)} = +3.9$) from this study, with high strontium (1,409 ppm; $^{87}Rb/^{86}Sr = 0.12$) and SiO_2 (64.13%) contents. Samples from the Bocşa massif (units 1, 2 and 3) are relatively clustered on the diagrams, except for two samples (95R15 and 98R02) of Bocşa 1. The three samples of Bocşa 1 display decreasing Sr_i with increasing SiO_2, at relatively constant $\epsilon_{Nd(t)}$ values. A similar relationship is observed for samples from the Tincova intrusion. The Sr_i versus Sr (Fig. 7B) and $\epsilon_{Nd(t)}$ versus Nd (Fig. 7D) diagrams show the same variations with SiO_2, as both elements are compatible (Fig. 4).

Discussion on magma origin and igneous evolution

A common fractionation trend ranging from 50 to 67% SiO_2, the general lack of cumulate textures, the absence of strong positive europium anomalies, and the smooth REE patterns support the hypothesis that the samples approximate liquid compositions, following a common liquid line of descent. However, the observed scatter in Sr_i and $\epsilon_{Nd(t)}$ values, and the occurrence of rounded mafic microgranular enclaves (MME) suggest that the seven intrusions resulted from differentiation of several

Table 5 Whole-rock major element (in wt%) and trace element (in ppm) data for the studied samples (Banat, Romania). *L.O.I.* Loss on ignition, *A.I.* agpaitic index, *OF-D* Ocna de Fier – Dognecea, *MN* Moldova Nouă, *Eu/Eu** europium anomaly. Sm and Nd contents were obtained by isotope dilution (see analytical methods for more details)

	Tincova				Bocşa 1			Bocşa 2			Bocşa 3		OF-D	Oraviţa						Ciclova		Sasca		MN
	98R18	98R22	98R20	98R23	95R15	98R02	95R13	95R09	95R11	95R07	98R13	98R16	98R04	98R10	98R05	98R07	98R08	98R09	95R04	98R12	98R11	98R24	98R26	98R27
SiO_2	60.98	63.60	64.83	66.91	50.12	54.94	64.78	63.86	64.45	65.71	61.91	66.50	62.66	48.44	56.66	63.42	63.91	64.13	64.53	54.37	59.6	62	62.63	63.10
TiO_2	0.64	0.52	0.55	0.48	0.64	0.88	0.51	0.50	0.52	0.48	0.59	0.45	0.61	0.93	0.64	0.50	0.48	0.50	0.48	0.84	0.50	0.53	0.48	0.54
Al_2O_3	16.06	16.14	15.92	15.55	15.37	18.65	15.29	15.07	15.32	16.59	15.25	15.36	15.64	16.79	16.62	15.20	15.68	15.42	15.71	16.44	16.30	16.09	16.11	16.24
$(Fe_2O_3)t$	5.46	4.47	4.69	3.72	7.81	7.35	4.46	4.65	4.44	4.13	4.97	3.74	5.33	10.27	6.13	4.93	4.52	4.59	4.52	8.16	6.10	4.63	4.26	4.51
MnO	0.10	0.08	0.09	0.06	0.14	0.12	0.07	0.09	0.09	0.05	0.10	0.08	0.09	0.15	0.08	0.03	0.05	0.06	0.06	0.15	0.10	0.06	0.05	0.07
MgO	3.39	2.35	2.60	2.09	4.87	2.58	1.71	1.94	1.94	1.76	3.07	2.23	3	7.45	4.83	2.87	2.60	2.46	2.52	4.46	4.03	2.54	2.47	2.68
CaO	4.55	3.73	4.45	3.61	13.28	6.55	3.86	4.07	3.76	4.09	4.99	3.78	4.98	11.51	6.52	3.96	4.39	4.40	4.44	8.11	5.66	4.71	5.13	5.26
Na_2O	4.77	5.06	4.28	4.49	2.65	3.77	4.20	4.14	4.10	4.48	4.26	4.19	3.96	1.96	4.21	3.68	4.28	4.40	4.19	3.89	4.18	4.75	4.42	5.18
K_2O	2.51	2.69	2.67	2.82	1.32	3.76	3.77	3.82	3.79	1.70	2.58	3.31	2.47	0.31	1.38	2.40	2.60	2.71	2.81	1.48	2.13	2.13	1.81	1.67
P_2O_5	0.15	0.19	0.12	0.13	0.39	0.59	0.20	0.21	0.19	0.19	0.17	0.12	0.23	0.58	0.26	0.20	0.18	0.18	0.15	0.25	0.32	0.15	0.15	0.16
L.O.I.	1.97	2.11	0.76	0.94	3.41	1.33	1.12	0.99	1.12	1.06	1.57	0.84	0.61	1.55	2.38	3.10	1.22	0.98	1.05	1.36	1.17	2.50	3.02	1.06
Total	100.57	100.92	100.96	100.80	99.99	100.52	99.97	99.34	99.70	100.26	99.45	100.59	99.57	99.95	99.72	100.28	99.91	99.85	100.46	99.50	100.10	100.08	100.53	100.47
Rb	84	111	97	102	43	92	139	157	133	65	95	121	88	182	73	117	106	59	88	90	46	87	63	67
Cs	2.59	2.75	2.67	2.23	7.15	2.77	5.36	5.57	4.89	4.21	2.20	2.34	4.24	6.79	6.35	12.9	6.31	3.55	5.2	4.63	3.97	3.09	3.23	3.27
Sr	642	507	480	420	1,328	766	561	577	552	624	536	423	555	1,286	555	463	509	1,409	503	638	892	565	697	544
Ba	601	575	558	554	357	530	534	522	562	465	648	482	658	847	304	468	515	679	553	580	452	507	568	532
V	118	89	110	78	142	114	69	70	60	64	127	94	97	46	124	95	88	197	57	139	210	96	104	115
Cr	43	30	52	31	26	16.6	14.6	14.3	13.8	14.1	42	26	33	11.8	53	27	21	16.7	17.3	34	23	35	33	29
Co	14.9	11.6	13.1	9.15	19	15.5	10.5	10.3	8.52	10.1	13.2	10.5	13	5	13.4	9.5	9.71	21	9.19	17.1	20	12.4	9.58	11.2
Ni	20	16.2	17.1	12.8	26	11.9	6.9	8.7	9	8.8	14.4	10.2	17	44	28	11.8	13	18.2	10.9	15.3	20	11.1	12.1	11.2
Zn	79	72	64	43	62	97	58	53	38	31	117	66	57	80	53	78	64	109	37	98	73	41	51	65
Ga	16.8	17.5	16.1	15.8	16.4	17.8	16.8	17.3	15.2	16.4	17.9	15.3	16.2	15.9	17.3	16.4	16.1	18.8	15.6	16.2	17.6	16.3	16.8	16.2
Zr	154	161	143	133	75	199	185	201	197	184	176	156	143	136	111	133	125	146	120	183	113	138	136	146
Hf	3.85	3.84	3.68	3.69	2.73	6.00	5.53	5.84	6.70	5.26	3.96	4.25	4.47	3.59	3.89	4.07	3.63	4.11	4.21	4.56	2.82	3.63	3.5	3.68
Zr/Hf	40	41.9	38.9	36	27.5	33.2	33.5	34.4	29.4	35	44.4	36.7	32	37.9	28.5	32.7	34.4	35.5	28.5	40.1	40.1	38	38.9	39.7
Nb	9.17	16.3	8.83	14.9	3.67	12.7	9.11	9.37	9.39	5.57	14.7	13.9	11	10.1	8.58	11.2	9.77	7.96	8.37	8.2	7.59	13.1	12.2	15.9
Ta	0.91	1.25	0.83	1.25	0.49	0.82	1.03	0.72	0.95	0.69	1.15	1.18	1.10	1.26	0.83	0.87	0.91	0.53	0.89	0.92	0.55	1.44	0.84	1.31
Nb/Ta	10.1	13	10.6	11.9	7.49	15.4	8.84	13	9.88	8.07	12.8	11.8	9.97	8.02	10.3	12.8	10.7	15	9.4	8.91	13.8	9.10	14.6	12.1
U	2.84	3.37	3.58	3.53	1.92	2.75	4.76	4.26	5.71	1.81	3.97	5	4.04	4.07	5.48	5.37	4.56	3.41	3.38	5.2	1.75	3.31	2.69	2.64
Th	11.2	11.5	13.6	12.7	6.12	9.27	21	14.7	19	5.10	18,5	28	22	18	12	13.9	13.7	21	16.5	20	7.22	11	11	9.19
U/Th	0.25	0.29	0.26	0.28	0.31	0.30	0.23	0.29	0.30	0.35	0.21	0.18	0.18	0.23	0.46	0.39	0.33	0.16	0.20	0.26	0.24	0.30	0.25	0.29
Pb	13.7	12.2	14.6	12.6	22	23	19.6	17.4	21	11.8	16.5	20	16.6	29	13.9	14.3	17.9	31	17	35	14.2	9.08	9.92	15.3
Y	18.5	19.9	17.1	18.4	21	28	21	15.1	16.5	10.1	24	19.7	17.9	20	26	21	16.4	24	14.6	22	24	19	18.1	22
La	31	31	31	35	30	36	35	36	35	26	38	48	34	44	36	28	29	47	36	37	29	28	28	26
Ce	54	57	51	59	56	75	70	59	63	41	69	67	61	81	68	54	47	89	54	65	51	48	50	47
Pr	5.93	6.28	5.32	6.11	6.83	9.54	7.75	6.46	7.01	4.64	7.72	6.91	6.75	8.82	7.66	6.14	5.37	10.5	5.85	7.61	6.66	5.41	5.46	5.14
Nd	23.5	24.2	21.6	23.1	54.6	40.7	31.8	26.4	27.6	19.3	28.4	25.3	28.1	28.7	30.8	25.6	21	42.7	23.8	26.3	31.9	21.4	22.7	20.8
Sm	4.43	4.43	4.01	4.06	10.43	8.22	5.92	4.74	5.03	3.48	5.28	4.45	5.27	6.44	5.85	5.04	4	7.50	4.28	5.38	5.88	3.99	4.18	4
Eu	1.02	0.93	0.91	0.97	1.49	1.99	1.19	1.09	1.24	1.10	1.32	1.03	1.36	0.99	1.65	1.25	1.01	1.90	1.13	1.45	1.41	1.05	1.08	1.03
Gd	3.73	3.64	2.82	3.01	4.79	7.44	5.07	4.61	4.55	3	3	3.70	4.72	4.77	5.58	4.31	3.39	6.56	4.10	4.59	3.91	2.36	2.87	2.62
Tb	0.46	0.43	0.40	0.41	0.77	1.10	0.79	0.61	0.74	0.42	0.54	0.42	0.71	0.62	0.75	0.70	0.56	0.92	0.57	0.69	0.65	0.47	0.39	0.42
Dy	2.70	2.61	2.14	2.46	3.80	5.01	3.56	2.89	3.22	2.26	2.95	2.49	3.17	3.18	3.92	3.56	2.67	3.76	2.91	3.27	3.15	2.62	2.50	2.82
Ho	0.63	0.58	0.53	0.54	0.78	1.05	0.74	0.64	0.73	0.44	0.68	0.62	0.67	0.7	0.99	0.82	0.54	0.82	0.77	0.69	0.73	0.57	0.60	0.67
Er	1.49	1.44	1.30	1.34	1.99	2.54	2.02	1.58	1.83	1.08	1.72	1.54	1.68	1.78	2.51	1.93	1.39	2.06	1.74	1.84	1.88	1.46	1.41	1.78
Tm	0.28	0.30	0.19	0.27	0.31	0.38	0.37	0.26	0.25	0.17	0.34	0.26	0.28	0.30	0.47	0.32	0.26	0.31	0.26	0.31	0.30	0.26	0.25	0.28
Yb	1.50	1.48	1.48	1.43	1.98	2.56	1.93	1.45	1.87	1	1.82	1.70	1.65	1.89	2.66	1.95	1.66	1.78	1.78	1.86	1.88	1.65	1.51	1.86
Lu	0.23	0.27	0.24	0.24	0.30	0.46	0.36	0.17	0.32	0.19	0.29	0.28	0.30	0.27	0.43	0.34	0.29	0.28	0.32	0.28	0.26	0.28	0.24	0.29
(La/Yb)n	15	15.2	15	17.5	11.02	10.08	13.14	18	13.26	18.4	14.9	20.4	14.9	16.9	9.58	10.2	12.7	18.9	14.4	14.2	11	12	13.1	10.1
Eu/Eu*	0.78	0.71	0.84	0.88	0.83	0.80	0.66	0.74	0.76	1.08	0.91	0.74	0.82	0.58	0.88	0.8	0.87	0.8	0.84	0.86	0.99	1.07	0.98	1.01
A.I.	0.66	0.70	0.62	0.67	0.38	0.55	0.72	0.73	0.71	0.56	0.64	0.68	0.59	0.21	0.51	0.57	0.63	0.66	0.63	0.49	0.56	0.63	0.57	0.64

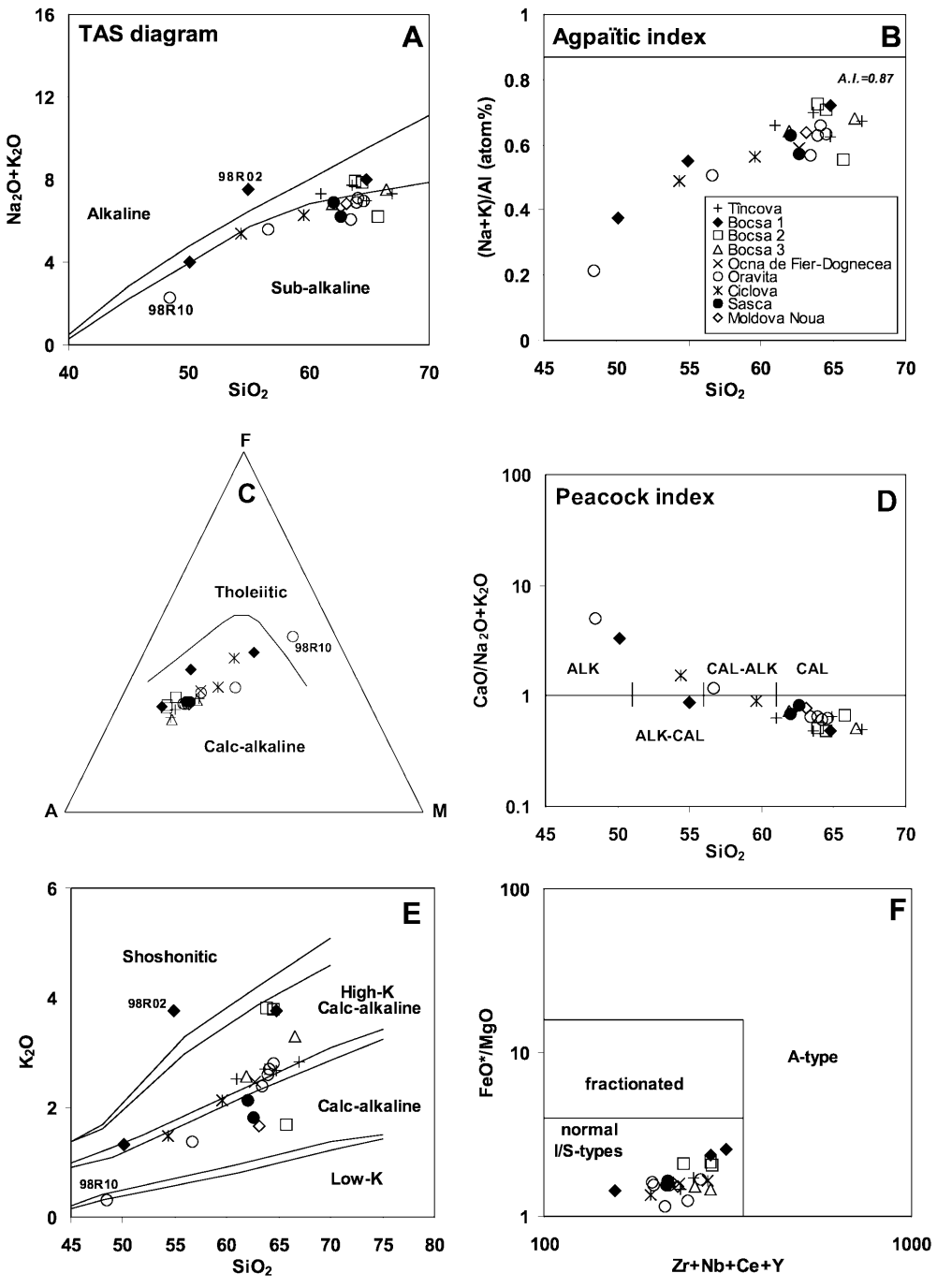

Fig. 3A–F Geochemical typology of the studied intrusions. **A** ($Na_2O + K_2O$) vs. SiO_2 (TAS diagram; divisions after Rickwood 1989). **B** (Na + K)/Al (atom%) vs. SiO_2 (agpaïtic index). A.I. = 0.87 is the minimum value for alkaline metaaluminous granitoids (Liégeois and Black 1987). **C** AFM diagram (division after Irvine and Baragar 1971). **D** CaO/($Na_2O + K_2O$) vs. SiO_2 (Peacock index; Brown 1981). **E** K_2O vs. SiO_2 (divisions after Rickwood 1989). **F** (FeO^*/MgO) vs. (Zr + Nb + Ce + Y) in ppm (FeO^* = total iron reported as FeO; Whalen et al. 1987). These diagrams show the calc-alkaline nature and the I-type affinity of the samples. The *legend* in **B** applies to all six diagrams

pulses of parental magma, but with similar/related major and trace element compositions.

Modelling of the liquid line of descent

Trends in variation diagrams can result either from fractional crystallisation or magma mixing. If mixing is the dominant differentiation process, then linear trends should be obtained in all variation diagrams. The strontium vs. rubidium diagram (Fig. 8A) shows an exponential decrease of strontium with differentiation (increasing rubidium content), indicating that fractional crystallisation was probably a major differentiation process. A negative correlation in a cobalt (compatible) vs. rubidium (incompatible) bilogarithmic diagram also supports this conclusion (Fig. 8B).

As an alternative to least squares regression using measured compositions of crystallising phases, we tried to test the fractionation hypothesis using the MELTS algorithm of Ghiorso and Sack (1995). The MELTS approach models the crystallisation of a magma for given conditions (temperature, pressure, magma composition and oxygen fugacity), based on a thermodynamic

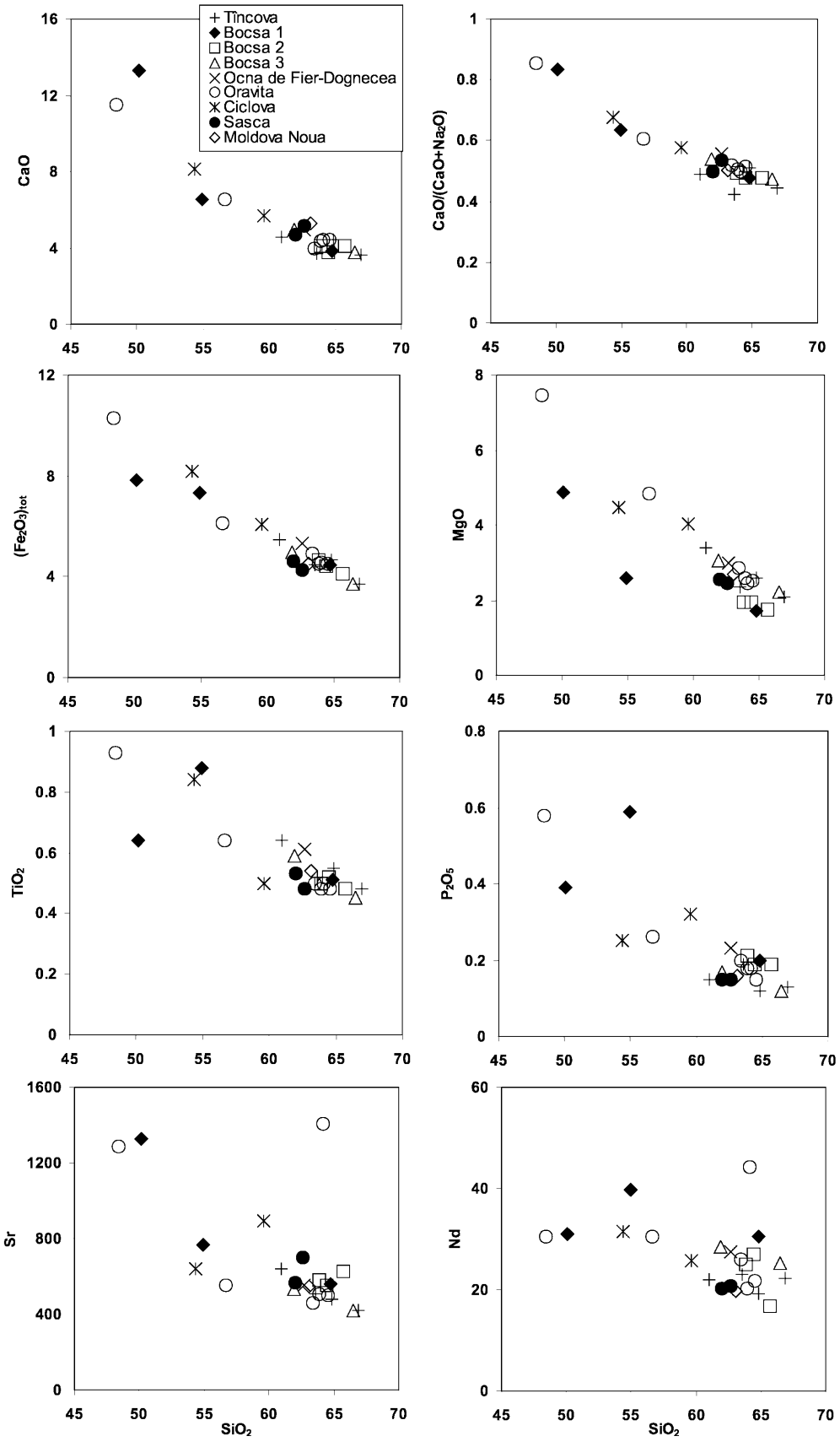

Fig. 4 Major (in wt%) and trace (in ppm) element variation diagrams (Harker diagrams). These diagrams show that the samples define one single trend even though they belong to seven distinct intrusions

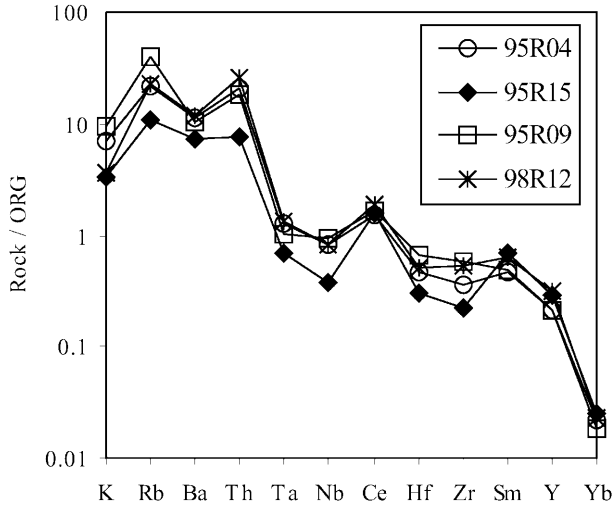

Fig. 5 Ocean ridge granite-normalised spidergrams after Pearce et al. (1984). All other samples fall in the restricted compositional range displayed in this diagram

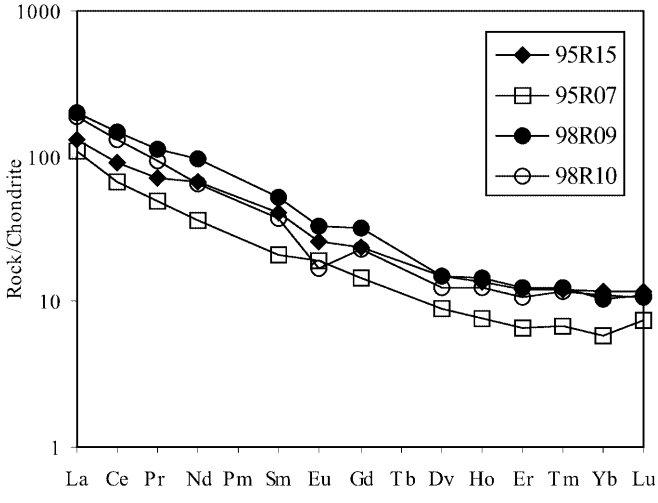

Fig. 6 Chondrite-normalised REE patterns (normalising values from Sun and McDonough 1989). All other samples fall in the restricted compositional range displayed in this diagram

description of silicate melt and precipitated minerals. Sample 98R12 was selected as having the closest composition to the common parental magma. Temperature and pressure were estimated from the data of Nicolescu and Cornell (1999). Using the amphibole-plagioclase geothermometer (Holland and Blundy 1994), they obtained a mean crystallisation temperature of 735 ± 75 °C for the Ocna de Fier – Dognecea granodiorite, and 722 ± 75 °C for the Bocşa 3 granodiorite. From the aluminium-in-hornblende geobarometer of Schmidt (1992), they estimated pressures of emplacement at 2.9 ± 0.6 kbar for Ocna de Fier – Dognecea, and 2.4 ± 0.6 kbar for Bocşa 3. Titanite is nearly ubiquitous in the studied samples, implying that magmas crystallised at an oxygen fugacity close to the Ni-NiO buffer (Wones 1989).

Modelling results (Table 7) are in approximate agreement with the petrographic sequence of crystallisation, indicating that the chosen starting composition and estimated conditions of crystallisation are plausible. Clinopyroxene is the liquidus phase at 1,150 °C, and plagioclase appears soon after, at 1,110 °C. The liquidus plagioclase is An_{66}, close to the optical determination of An_{70} (see petrography section). Only titano-magnetite is predicted, whereas in our samples both magnetite and ilmenite were observed, but the model is known for poor prediction of Fe-Ti oxide saturation (Toplis and Carroll 1996). Titanite does not appear with the MELTS simulation; this may result from excessive ulvöspinel in magnetite. The MELTS calculations also predict the saturation of cummingtonite instead of hornblende, and amphibole after biotite saturation, opposite to the observed sequence. The proportion of plagioclase in the calculated cumulates (Table 7) is high and in apparent contradiction with the weak, negative europium anomalies ($Eu/Eu^* = 0.7$ to 0.9) displayed by the samples (Fig. 6). However, when plagioclase crystallises cotectically with other phases (clinopyroxene and apatite here) having higher $D_{REE}^{min/liq}$, then the influence of plagioclase on the resulting REE pattern of the residual liquid is drastically decreased (Vander Auwera et al. 1998a).

Evolution of the isotopic signatures during differentiation

The isotopic data presented in Fig. 7 suggest that some contamination, mostly affecting Sr_i, occurred during the differentiation of the Oraviţa, Bocşa 3 and Ocna de Fier – Dognecea intrusions. The Sr_i of sample 98R09 (from the Oraviţa intrusion) and of samples from Bocşa 1 and Tincova do not fit a differentiation trend because the most evolved samples display the most juvenile isotopic signatures. These samples would thus consist of more isotopically primitive magma influxes, which could have continued differentiating in an intermediate magma chamber without undergoing important contamination. The least differentiated samples of the studied intrusions, 98R10 from Oraviţa ($SiO_2 = 48.44\%$) and 95R15 from Bocşa 1 ($SiO_2 = 50.12\%$), have very distinct Sr_i (98R10: 0.704167, 95R15: 0.705450) and $\epsilon_{Nd(t)}$ values (98R10: +2.9, 95R15: +1.8). Moreover, the very high strontium content of sample 95R15 (1,328 ppm), together with its low SiO_2 content, preclude that an early magma contamination process induced its high Sr_i. It seems, therefore, more plausible that the observed variability is inherited from a heterogeneous source.

Potential magma sources

Most of the mafic samples plot on the boundary between the calc-alkaline and high-potassium calc-alkaline fields (Fig. 3E), indicating that the K_2O enrichment was already important at the beginning of the liquid line of descent. This suggests that the K_2O enrichment is source inherited (Roberts and Clemens 1993; Lié-

Table 6 Strontium and neodymium isotopic data for the studied samples (Banat, Romania). *OF-D* Ocna de Fier – Dognecea, *MN* Moldova Nouă. Sm and Nd contents were obtained by isotope dilution (refer to the analytical methods for more details). See Steiger and Jäger (1977) for the values of the used radioactive decay constants

Intrusion	Sample	SiO_2 (%)	Rb (ppm)	Sr (ppm)	Sm (ppm)	Nd (ppm)	$^{87}Rb/^{86}Sr$[a]	$^{87}Sr/^{86}Sr$ (measured, 2 σ)	$^{87}Sr/^{86}Sr$ (80 Ma)	ϵ_{Sr} (0)	ϵ_{Sr} (80 Ma)	$^{147}Sm/^{144}Nd$	$^{143}Nd/^{144}Nd$ (measured, 2 σ)	T_{DM} (Ga)	ϵ_{Nd} (0)	ϵ_{Nd} (80 Ma)
Tincova	98R18	60.98	84	642	4.43	23.5	0.378	0.706236 ± 12	0.705806	24.6	19.9	0.1140	0.512636 ± 11	0.638	0	0.8
	98R22	63.60	111	507	4.43	24.2	0.633	0.706016 ± 11	0.705296	21.5	12.6	0.1107	0.512583 ± 9	0.694	–1.1	–0.2
	98R20	64.83	97	480	4.01	21.6	0.584	0.705610 ± 12	0.704946	15.8	7.7	0.1122	0.512678 ± 10	0.567	0.8	1.6
	98R23	66.91	102	420	4.06	23.1	0.702	0.705775 ± 13	0.704977	18.1	8.1	0.1063	0.512613 ± 7	0.625	–0.5	0.4
Bocşa 1	95R15	50.12	43	1,328	10.43	54.6	0.094	0.705556 ± 13	0.705450	15.0	14.8	0.1155	0.512686 ± 8	0.573	0.9	1.8
	98R02	54.94	92	766	8.22	40.7	0.347	0.705458 ± 11	0.705063	13.6	9.3	0.1221	0.512611 ± 9	0.732	–0.5	0.2
	95R13	64.78	139	561	5.92	31.8	0.717	0.705651 ± 15	0.704836	16.3	6.1	0.1125	0.512646 ± 8	0.615	0.2	1.0
Bocşa 2	95R09	63.86	157	577	4.74	26.4	0.787	0.705759 ± 11	0.704864	17.9	6.5	0.1085	0.512655 ± 8	0.580	0.3	1.2
	95R11	64.45	133	552	5.03	27.6	0.697	0.705698 ± 11	0.704906	17.0	7.1	0.1102	0.512663 ± 7	0.577	0.5	1.4
	95R07	65.71	65	624	3.48	19.3	0.301	0.705257 ± 13	0.704915	10.7	7.2	0.1090	0.512627 ± 8	0.621	–0.2	0.7
Bocşa 3	98R13	61.91	95	536	5.28	28.4	0.513	0.705382 ± 12	0.704799	12.5	5.6	0.1124	0.512655 ± 7	0.601	0.3	1.2
	98R16	66.50	121	423	4.45	25.3	0.827	0.705999 ± 15	0.705059	21.3	9.3	0.1063	0.512634 ± 8	0.597	–0.1	0.8
OF-D	98R04	62.66	88	555	5.27	28.1	0.459	0.705485 ± 11	0.704964	14.0	7.9	0.1134	0.512660 ± 7	0.599	0.4	1.3
Oraviţa	98R10	48.44	182	1,286	6.44	28.7	0.409	0.704632 ± 11	0.704167	1.9	–3.4	0.1357	0.512757 ± 9	0.581	2.3	2.9
	98R05	56.66	73	555	5.85	30.8	0.380	0.705286 ± 10	0.704854	11.2	6.4	0.1148	0.512683 ± 9	0.573	0.9	1.7
	98R07	63.42	117	463	5.04	25.6	0.731	0.705818 ± 11	0.704987	18.7	8.3	0.1190	0.512681 ± 8	0.601	0.8	1.6
	98R08	63.91	106	509	4.00	21.0	0.602	0.705611 ± 12	0.704926	15.8	7.4	0.1151	0.512670 ± 9	0.595	0.6	1.5
	98R09	64.13	59	1,409	7.50	42.7	0.121	0.704421 ± 12	0.704283	–1.1	–1.7	0.1062	0.512789 ± 8	0.385	2.9	3.9
	95R04	64.53	88	503	4.28	23.8	0.506	0.705563 ± 12	0.704988	15.1	8.3	0.1087	0.512649 ± 7	0.589	0.2	1.1
Ciclova	98R12	54.37	90	638	5.38	26.3	0.408	0.704676 ± 13	0.704212	2.5	–2.8	0.1237	0.512700 ± 7	0.600	1.2	2.0
	98R11	59.60	46	892	5.88	31.9	0.149	0.704729 ± 12	0.704559	3.3	2.2	0.1114	0.512755 ± 8	0.452	2.3	3.2
Sasca	98R24	62.00	87	565	3.99	21.4	0.445	0.705510 ± 12	0.705004	14.3	8.5	0.1127	0.512659 ± 9	0.597	0.4	1.3
	98R26	62.63	63	697	4,18	22,7	0.261	0.704814 ± 12	0.704517	4.5	1.8	0.1113	0.512734 ± 6	0.482	1.9	2.7
MN	98R27	63.10	67	544	4.00	20.8	0.356	0.705116 ± 13	0.704711	8.7	4.3	0.1163	0.512779 ± 14	0.437	2.8	3.6

[a] $(^{87}Sr/^{86}Sr)_{UR} = 0.7045$ and $(^{87}Rb/^{86}Sr)_{UR} = 0.0827$ (De Paolo and Wasserburg 1976). $(^{143}Nd/^{144}Nd)_{CHUR} = 0.512638$ and $(^{147}Sm/^{144}Nd)_{CHUR} = 0.1966$ (Jacobsen and Wasserburg 1980). Equation used for depleted mantle evolution: ϵ_{Nd} (T in Ga) = $0.25T^2 - 3T + 8.5$ (De Paolo 1981). UR: uniform reservoir; CHUR: chondriticuniform reservoir

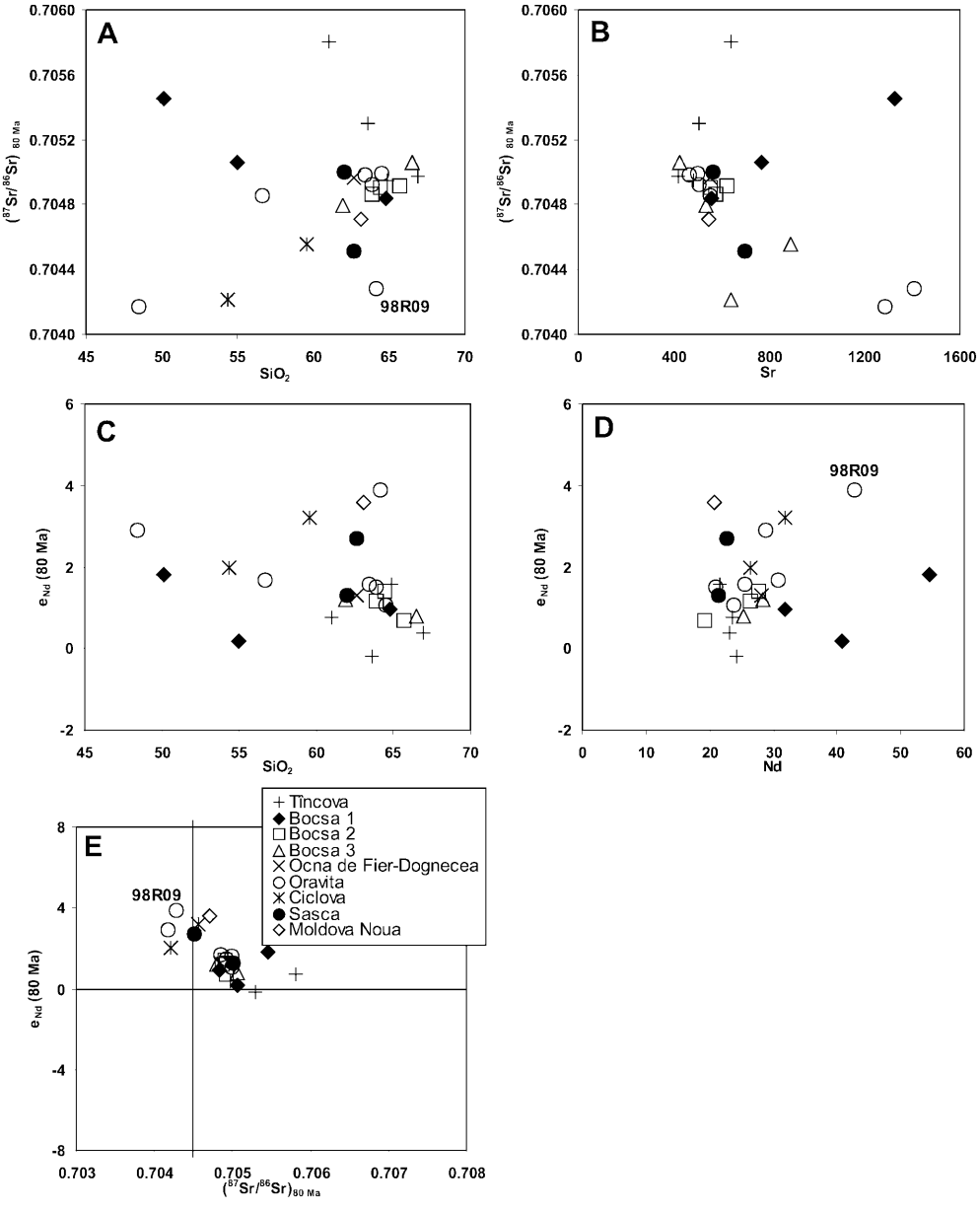

Fig. 7A–E Isotopic ratios have been corrected for in situ decay considering an age of 80 Ma. **A** Sr_i vs. SiO_2 (in wt%), **B** Sr_i vs. Sr (in ppm), **C** $\epsilon_{Nd(t)}$ vs. SiO_2 (in wt%), and **D** $\epsilon_{Nd(t)}$ vs. Nd (in ppm). These four diagrams suggest that a minor assimilation – fractional crystallisation (AFC) event characterised the Oraviţa, Bocşa 3 and Ocna de Fier – Dognecea intrusions. **E** $\epsilon_{Nd(t)}$ vs. Sr_i. This diagram shows that the magma source was depleted in neodymium and enriched in strontium. The *legend* displayed in **E** applies to all five diagrams

geois et al. 1998). The positive $\epsilon_{Nd(t)}$ values and relatively low Sr_i values (Table 6) imply that the source of most samples was depleted in neodymium and slightly enriched in rubidium, possibly consisting of a heterogeneous mantle or a young mafic lower crust derived from it (Liégeois et al. 1998). This heterogeneity and LILE enrichment could be due to mantle metasomatism during an older subduction event. Decoupling of neodymium and rubidium during metasomatism of the mantle wedge could result either from the composition of the transporting agent (aqueous fluid versus hydrated silicate melt) or from its interaction with the lithospheric mantle.

The pre-intrusion subduction event could be Early Cretaceous or older. Very similar T_{DM} model ages (ca. 600 Ma; except for samples 98R09, 98R11, 98R26 and 98R27 with lower values; Table 6) could represent the time of extraction of a protolith from a selectively metasomatised mantle. This protolith may have remained isolated in the lower crust until about 80 Ma, when partial melting occurred and generated the parental magmas for the intrusions. The T_{CHUR} model ages are systematically negative, or lower than crystallisation ages, and have not been further considered. During the Late Cretaceous, subduction-related mantle magmas may have underplated the lower crust and caused partial melting of the variably enriched protolith, following a MASH-type process (melting – assimilation – storage – homogenisation; Hildreth and Moorbath 1988). The felsic magmas typically resulting from this process would explain the abundance of granodiorites within the BMMB and, due to their higher densities relative to average crust, the relative scarcity of mafic compositions in Banat.

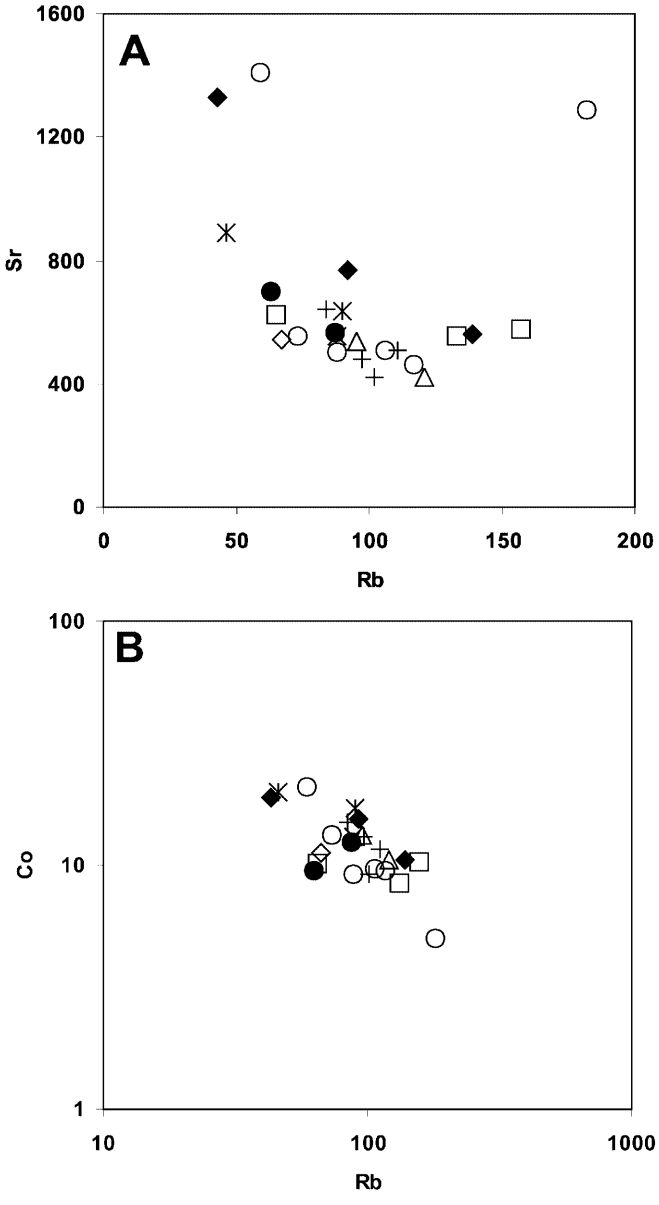

Fig. 8 **A** Sr vs. Rb (in ppm) diagram showing an exponential decrease of strontium with increasing rubidium content. **B** Co vs. Rb (in ppm) log-log diagram showing a negative correlation. Both diagrams suggest that fractional crystallisation was the dominant differentiation process (same symbols as in previous figures)

Consequences and conclusions for regional metallogeny

In this study, we set out to test whether or not regional differences of deposit characteristics in the Banat region of Romania were related to differences in magma composition and origin, and thus might have large-scale geodynamic causes. The new isotopic and geochemical results, and their regional geologic context, can be discussed with regard to four factors, which probably all contributed to the style and metal content of magmatic-hydrothermal ore deposits in the Romanian part of the BMMB. These are (1) the origin and composition of the subduction-related magmas, (2) the depth of erosion later affecting deposit preservation, (3) the nature of host-rock types, and (4) deposit-scale zoning due to successive mineral precipitation from fluids.

The *composition and origin of magmas* seems to have some influence on whether or not metalliferous deposits are present. Russo-Săndulescu and Berza (1979) and Russo-Săndulescu et al. (1984) subdivided the intrusions from Banat into a shoshonitic group and a calc-alkaline group. The shoshonitic group includes the Surduc and Bocşa intrusions (units 1 and 2). No ore deposits have been recognised in association with these two intrusions. The second group has a calc-alkaline to high-potassium calc-alkaline affinity and includes the Tincova, Bocşa 3, Ocna de Fier – Dognecea, Oraviţa, Ciclova, Sasca and Moldova Nouă intrusions. All of these are associated with ore deposits containing economic, or at least some, copper and molybdenum mineralisation. However, no significant geochemical differences seem to exist among these calc-alkaline to high-potassium calc-alkaline intrusions. The geochemical data define a single trend in major and trace element variation diagrams, consistent with fractional crystallisation of several pulses of parental magma having similar compositions. The strontium and neodymium isotopic compositions of the intrusions do not significantly differ, although minor variations exist, probably indicating a slightly heterogeneous mantle or lower crustal source. In particular, there are no regionally systematic, compositional or isotopic differences in the magmas along the studied part of the BMMB which could suggest a deepening of the subduction zone towards the north-west (Vlad 1979, 1997). Variation in the chemistry (major and trace elements, strontium and neodymium isotopic compositions) of the calc-alkaline magmas which formed these intrusions, therefore, seems to be an unlikely cause for differences in the deposit types between northern Banat, where exclusively skarn deposits occur (mostly with lead, zinc and iron), and southern Banat and Timok (Serbia) where porphyry-style copper-molybdenum deposits occur, as well as skarns.

The *depth of post-mineralisation erosion* determines which of the deposit types developed in association with the calc-alkaline magmas are likely to be present in various parts of the Banat region. Erosion depth probably contributes to the exclusive occurrence of skarns in northern Banat where large intrusions are exposed, which mainly display coarse-grained textures (Tincova, Bocşa 3, Ocna de Fier – Dognecea, and also smaller parts of Oraviţa, Ciclova and Sasca). Pressure estimates of 2.4 and 2.9 kbar for the Bocşa 3 and Ocna de Fier – Dognecea samples respectively (Nicolescu and Cornell 1999) indicate mid-crustal depths of emplacement of approximately 10 km. In southern Banat, smaller stocks and apophyses of shallower-seated intrusions, relative to northern Banat, are exposed. These apophyses exhibit dominant porphyric

Table 7 Results obtained with the MELTS algorithm (Ghiorso and Sack 1995) for modelling variation in major element content of melt during fractional crystallization. *F* liquid fraction, *amp* amphibole, *an* anorthite, *ap* apatite, *bio* biotite, *cpx* clinopyroxene, *en* enstatite, *fs* ferrosilite, *mt* magnetite, *pl* plagioclase, *qz* quartz, *sp* spinel, *uvsp* ulvöspinel, *wo* wollastonite

Sample 98R12: Ni-NiO buffer
Increment 10 °C, water content 1.38%
Start crystallisation temperature: 1,250 °C, end crystallisation temperature: 600 °C

Crystallisation temperature (°C)	Phase	Crystallisation temperature (°C)	Calculated cumulate	F
1,150	Cpx ($Wo_{38}En_{50}Fs_{12}$: augite)	1,150	100% cpx	0.98
1,110	Cpx – pl (An_{66}: labradorite)	1,110	87.2% cpx + 12.8% pl	0.86
1,060	Cpx – pl – mt ($Mt_{50}Sp_{23}Uvsp_{27}$: titano-magnetite)	1,060	58% cpx + 41.4% pl + 0.6% mt	0.65
940	Cpx – pl – mt – ap	940	38.8% cpx + 55.4% pl + 5.7% mt + 0.03% ap	0.35
840	Cpx – pl – mt – ap – bio (phlogopite)	840	36.2% cpx + 58.6% pl + 4.7% mt + 0.16% ap + 0.28% bio	0.23
760	Cpx – pl – mt – ap – bio – H_2O	760	37.3% cpx + 60.6% pl + 0.6% mt + 0.34% ap + 0.37% bio + 0.76% H_2O	0.09
690	Cpx – pl – mt – ap – bio – H_2O – amp (cummingtonite)	700	37% cpx + 61.5% pl + 0.38% ap + 1.1% H_2O	0.05
680	Cpx – pl – mt – ap – bio – H_2O – amp – qz			

Final liquid SiO_2 content: 67.07%

textures with a medium- to fine-grained groundmass (Oraviţa, Ciclova, Sasca and Moldova Nouă). At Krepoljin (Serbia, Fig. 1), 50 km south of the Danube, dacitic dykes even intrude to subvolcanic depth (Karamata et al. 1997a). This indicates a general trend of decreasing erosion from north to south, which probably contributed to the preservation of porphyry-style mineralisation only in the southern area. Porphyry deposits could have developed in northern Banat but they would thus have been eroded away. A subeconomic stockwork mineralisation formed in association with the Oraviţa intrusion, the latter being located at the limit between northern and southern Banat, and Cioflica and Vlad (1980) considered that it represents "the root zone of an eroded porphyry molybdenum deposit".

The *nature of the host rocks*, notably the occurrence of carbonates, is controlled by Mesozoic sedimentation and then the nappe tectonics which preceded the intrusion of calc-alkaline magmas along N-S crustal lineaments. A first band of Mesozoic carbonates belonging to the Supragetic Upper Jurassic-Lower Cretaceous, NE-SW-trending cover of the Bocşa Nappe (Iancu 1985) is intruded in Ocna de Fier by the Bocşa 3 and Ocna de Fier – Dognecea intrusions. A more than 100-km-long second band of Mesozoic limestones outcrops between Reşiţa and Moldova Nouă, and is locally represented by Triassic carbonates from the Sasca-Gornjak Nappe (Fig. 1) as well as, more commonly, by carbonates belonging to the Upper Jurassic-Lower Cretaceous cover of the Getic nappes. In Romania, between Oraviţa and Moldova Nouă, and in Serbia (Ridanj-Krepoljin area), this band is cut by countless calc-alkaline intrusions ranging from gabbro (basalt) to granodiorite (dacite). Within both these carbonates bands, mafic compositions (mainly gabbroic bodies) have generated barren high-temperature calcic skarns (e.g. gehlenite- and mellilite-bearing skarns from Oraviţa and Ciclova, Marincea and Dumitras 2001) whereas granodiorites have induced medium-temperature calcic (mainly diopside-/hedenbergite-, wollastonite- and grandite-bearing) skarns and extensive mineralisations, preferentially located at the carbonate/crystalline schist contacts (i.e. iron (copper) deposits at Ocna de Fier – Dognecea: von Cotta 1864; Codarcea 1931; Vlad 1974; Cook and Ciobanu 2001) or at the carbonate/intrusion contacts (e.g. copper deposits at Sasca, Ciclova and Moldova Nouă: von Cotta 1864; Gheorghiţă 1975; Gheorgiţescu 1975; Constantinescu 1980; Ilinca et al. 1993; lead-zinc ores associated at Dognecea: Vlad 1974; Cook and Ciobanu 2001).

Precipitation mechanisms for ore minerals, which depend on pressure-temperature conditions, as well as chemical wall-rock reactions, finally contributed to variations in ore mineralogy in skarns at the deposit to district scale. An example is the zoning from an iron- and copper-rich skarn at the Ocna de Fier deposit to the lead-zinc ores at the more peripheral Dognecea deposit (Codarcea 1931; Vlad 1974; Ciobanu et al. 2002, this volume).

In summary, the ore deposits associated with magmatism which took place in the Banat region are partly controlled by the composition and combined mantle and crustal source history of the magmas, as indicated by a restriction of ore deposits to the main calc-alkaline group of intrusions. Even though this indicates an igneous derivation of the ore fluids and the metals they transport, the style of ore deposits and their final metal content is equally dependent on the smaller-scale geo-

logic setting of the ore district and the individual deposits.

Acknowledgements The help of G. Bologne and G. Delhaze for chemical analyses and sample preparation respectively was greatly appreciated. C. Bosque is thanked for her help during the preparation of the samples for isotopic analyses. M. Bernard is also thanked for his help during the acquisition process of the isotopic data. Dr. V. Iancu is warmly thanked for her help with the map drawing. Drs. R. Goldfarb, W. Halter and C. Heinrich as well as two anonymous reviewers made valuable comments which helped improve the manuscript. We would also like to thank the Geological Institute of Romania (GIR) for providing logistical support for the field work done in September 1998 and for giving us the precise latitude-longitude co-ordinates of the studied samples. A. Dupont is currently supported by an FRIA (Fonds pour la Formation à la Recherche dans l'Industrie et dans l'Agriculture) Ph.D. fellowship.

References

Andrei J, Cioflica G, Calota C, Jude R, Lupulescu M (1988) The structural model of banatitic magmatites in the Tincova area (Poiana Rusca Mts.) and its metallogenetic implications. Rev Roum Géol Géophys Géogr Géol 32: 45–54

Arsovski M, Dumurdžanov N (1995) Alpine tectonic evolution of the Vardar zone and its place in the Balkan region. Geol Maced 9: 15-22

Berza T (1997) A hundred years of tectonic studies in South Carpathians: The state of the art. In: Grubić A, Berza T (eds) Geology of Djerdap area. Geoinstitute Belgrade, pp 271–276

Berza T (1999) Tectonic setting of the Late Cretaceous Volcano-Plutonic Belt from Carpathians to Balkans. EUG X, J Conf Abstr 4: 469

Berza T, Constantinescu E, Vlad Ş-N (1998) Upper-Cretaceous magmatic series and associated mineralisation in the Carpathian – Balkan orogen. Resour Geol 48(4):291-306

Blanckenburg F von, Davies JH (1995) Slab breakoff: a model for syncollisional magmatism and tectonics in the Alps. Tectonics 14(1):120–131

Boccaletti M, Manetti P, Peccerillo A (1974) The Balkanids as an instance of Back-Arc Thrust Belt: Possible relation with the Hellenids. Geol Soc Am Bull 85:1077–1084

Boccaletti M, Manetti P, Peccerillo A, Stanisheva-Vassilieva G (1978) Late Cretaceous high-potassium volcanism in eastern Srednogorie, Bulgaria. Geol Soc Am Bull 89:439–447

Bologne G, Duchesne J-C (1991) X-ray fluorescence spectrometry analyses of silicate rocks: precision and exactitude (in French). Serv Géol Belg Prof Pap 249: 1–11

Brown GC (1981) Space and time in granite plutonism. Philos Trans R Soc Lond Ser A 301:321–336

Burchfiel BC (1980) Eastern European alpine system and the Carpathian orocline as an example of collision tectonics. Tectonophysics 63:31–61

Chappell BW, White AJR (1974) Two contrasting granite types. Pac Geol 8:173–174

Ciobanu CL, Cook NJ, Stein H (2002) Regional setting and geochronology of the Upper Cretaceous Banatitic Magmatic and Metallogenetic Belt. Miner Deposita (in press). DOI 10.1007/s00126-002-0272-9

Cioflica G (1989) Copper mineralisation related to Upper Cretaceous-Paleogene magmatites in Romania. Rev Roum Géol Géophys Géogr Géol 33:13–24

Cioflica G, Vlad Ş-N (1973) The correlation of Laramian metallogenic events belonging to the Carpatho-Balkan area. Rev Roum Géol Géophys Géogr Géol 17(2):217–224

Cioflica G, Vlad Ş-N (1980) Copper sulphide deposits related to Laramian magmatism in Romania. In: Jankovic S, Sillitoe RH (eds) Proc Int Symp European Copper Deposits, Belgrade, 1980. Spec Publ Soc Geol Appl Miner Deposits 1, pp 67–72

Cioflica G, Jude R, Lupulescu M, Ducea M (1996) Lower crustal origin of the Late Cretaceous-Eocene arc magmatism in the western part of the South Carpathians, Romania. In: Knežević V, Krstić B (eds) Terranes of Serbia. University of Belgrade, pp 103–107

Cioflica G, Jude R, Lupulescu M (1997) Late Cretaceous-Eocene arc magmatism related porphyry-type deposits in Romania. Rev Roum Géol Géophys Géogr Géol 41:3–18

Codarcea A (1931) Geological and petrographical study of the Ocna de Fier-Bocşa Montană area (Banat, Roumanie) (in Romanian). An Inst Geol Rom 15:261–424

Constantinescu E (1980) Mineralogy and genesis of the Sasca Montană skarn deposit (in Romanian). RS România, Bucharest

Cook N, Ciobanu C (2001) Paragenesis of copper-iron ores from Ocna de Fier – Dognecea (Romania), typifying fluid plume mineralization in a proximal skarn setting. Mineral Mag 65(3):351–372

Cotta B von (1864) About eruptive rocks and ore deposits from Banat and Serbia (in German). V Braunmüller, Vienna

Debon F, Lefort P (1983) A chemical-mineralogical classification of common plutonic rocks and associations. Trans R Soc Edinb Earth Sci 73:135–149

De Paolo DJ (1981) Neodymium isotopes in the Colorado Front Range and crust-mantle evolution in the Proterozoic. Nature 291:193–196

De Paolo DJ, Wasserburg GJ (1976) Inferences about magma sources and mantle structure from variations of $^{143}Nd/^{144}Nd$. Geophys Res Lett 3:743–746

Divljan M, Karamata S (1967) Eruptive rocks from the Ridanj-Krepoljin zone. In: Cretaceous-Tertiary magmatic rocks from Yugoslav Carpatho-Balkanides (in French). Acta Geol Acad Sci Hung 11(1–2):131–135

Djordjević M, Banješević M, Ralević B, Miličić M (1997) Mesozoic magmatism of Djerdap Area. In: Grubić A, Berza T (eds) Geology of Djerdap area. Geoinstitut Belgrade, pp 121–128

Drovenik M, Djordjević M, Antonijević I, Mičić I (1967) Magmatic rocks from the Timok eruptive area (in French). In: Cretaceous-Tertiary magmatic rocks from Yugoslav Carpatho-Balkanides. Acta Geol Acad Sci Hung 11(1–3):115–129

Gheorgiţa I (1975) Mineralogical and petrographical study of the Moldova Nouă region (Suvorov-Valea Mare area) (in Romanian). St Tehn Econ Inst Geol Geof, Bucharest, 1(11):1–188

Gheorgiţescu D (1975) Mineralogical and geochemical study of a thermal contact and metasomatic formation from Oraviţa (Cosoviţa) (in Romanian). DS Inst Geol Geof 61(1):59–103

Ghiorso MS, Sack RO (1995) Chemical mass-transfer in magmatic processes. IV. A revised and internally consistent thermodynamic model for the interpolation and extrapolation of liquid-solid equilibria in magmatic systems at elevated temperatures and pressures. Contrib Mineral Petrol 119:197–212

Grubić A (1974) Eastern Serbia in the light of the new global tectonics: consequences of this model for the interpretation of the tectonics of the Northern Branch of the Alpides. In: Karamata S (ed) Metallogeny and concepts of the geotectonic development of Yugoslavia. Geoinstitut Belgrade, pp 179–212

Hildreth W, Moorbath S (1988) Crustal contributions to arc magmatism in the Andes of Central Chile. Contrib Mineral Petrol 98:455–489

Holland T, Blundy J (1994) Non-ideal interactions in calcic amphiboles and their bearing on amphibole-plagioclase thermometry. Contrib Mineral Petrol 116:433–447

Iancu V (1985) Lower Supragetic nappes of the Banat, Moniom-Dognecea zone. DS Inst Geol Geof 69(5):31–36

Iancu V (1986) Supragetic and Infragetic structural units of western South Carpathians (in French). DS Inst Geol Geof 70–71(5):109–127

Ilinca G, Marincea Ş, Russo-Săndulescu D, Iancu V, Seghedi I (1993) Mineral occurrences in south-western Banat, Romania. Rom J Mineral 76(2):1–40

Irvine TN, Baragar WRA (1971) A guide to the chemical classification of the common volcanic rocks. Can J Earth Sci 8:523–548

Ishihara S (1977) The magnetite-series and ilmenite-series granitic rocks. Mining Geol 27:293–305
Jacobsen SB, Wasserburg GJ (1980) Sm-Nd evolution of chondrites. Earth Planet Sci Lett 50:139–155
Janković S (1997) The Carpatho-Balkanides and adjacent area: a sector of the Tethyan Eurasian metallogenetic belt. Miner Deposita 32:426–433
Karamata S, Knežević V, Pećskay Z, Djordjević M (1997a) Magmatism and metallogeny of the Ridanj-Krepoljin belt (eastern Serbia) and their correlation with northern and eastern analogues. Miner Deposita 32:452–458
Karamata S, Krstić B, Dimitrijević D, Dimitrijević MN, Knežević V, Stojanov R, Filipović I (1997b) Terranes between the Moesian plate and the Adriatic Sea. In: Papanikolau DJ, Ebner F (eds) Paleozoic geodynamic domains and their alpidic evolution in the Tethys, IGCP Project No 276. Ann Géol Pays Helléniques, Athens, 1ère Sér, XXVII, pp 429–478
Kräutner HG (1997) Alpine and pre-alpine terranes in the Romanian Carpathians and Apuseni Mts. In: Papanikolau DJ, Ebner F (eds) Paleozoic geodynamic domains and their alpidic evolution in the Tethys, IGCP Project No 276. Ann Géol Pays Helléniques, Athens, 1ère Sér, XXVII, pp 331–400
Liégeois JP, Black R (1987) Alkaline magmatism subsequent to collision in the Pan-African belt of the Adrar des Iforas (Mali). In: Fitton JG, Upton BGJ (eds) Alkaline igneous rocks. Geol Soc Spec Publ 30:381–401
Liégeois JP, Berza T, Tatu M, Duchesne J-C (1996) The Neoproterozoic Pan-African basement from the Alpine Lower Danubian nappe system (South Carpathians, Romania). Precambrian Res 80:281–301
Liégeois JP, Navez J, Hertogen J, Black R (1998) Contrasting origin of post-collisional high-K calc-alkaline and shoshonitic versus alkaline and peralkaline granitoids. The use of sliding normalization. Lithos 45:1–28
Marincea Ş, Dumitras D (2001) Mineralogical data on three endoskarn zones of the high-temperature banatitic skarns from Romania. Rom J Miner Deposits 79(2):66–67
Nicolescu S, Cornell DH (1999) P-T conditions during skarn formation in the Ocna de Fier ore district, Romania. Miner Deposita 34:730–742
Nicolescu S, Cornell DH, Bojar A-V (1999) Age and tectonic setting of Bocşa and Ocna de Fier-Dognecea granodiorites (southwest Romania) and of associated skarn mineralisation. Miner Deposita 34:743–753
O'Nions RK, Hamilton PJ, Evensen NM (1977) Variations in $^{143}Nd/^{144}Nd$ and $^{87}Sr/^{86}Sr$ ratios in oceanic basalts. Earth Planet Sci Lett 34:13–22
Pearce JA, Harris NBW, Tindle AG (1984) Trace element discrimination diagrams for the tectonic interpretation of granitic rocks. J Petrol 25:956–983
Pin C, Bassin C (1992) Evaluation of a strontium-specific extraction chromatographic method for isotopic analysis in geological materials. Anal Chim Acta 269:249–255
Pin C, Santos Zalduegui JF (1997) Sequential separation of light rare-earth elements, thorium and uranium by miniaturized extraction chromatography: application to isotopic analyses of silicate rocks. Anal Chim Acta 339:79–89
Popov PN (1981) Magmatectonic features of the Banat-Srednogorie Belt. Geol Balcanica 11(2):43–72
Popov PN (1987) Tectonics of the Banat-Srednogorie Rift. Tectonophysics 143:209–216
Popov PN (1996) Characteristic features of the Banat-Srednogorie metallogenic zone. In: Plate tectonic aspects of the Alpine Metallogeny in the Carpatho-Balkan region. IGCP Proj No 356 Annu Meet, Sofia, 1996, vol 1, pp 137–154
Rădulescu DP, Săndulescu M (1973) The plate tectonics concept and the geological structure of the Carpathians. Tectonophysics 16:155-161
Ratschbacher L, Linzer H-G, Moser F, Strusievicz R-O, Bedelean H, Har N, Mogos P-A (1993) Cretaceous to Miocene thrusting and wrenching along the Central South Carpathians due to a corner effect during collision and orocline formation. Tectonics 12(4):855–873
Rickwood PC (1989) Boundary lines within petrologic diagrams which use oxides of major and minor elements. Lithos 22:247–263
Roberts MP, Clemens JD (1993) Origin of high-potassium, calc-alkaline, I-type granitoids. Geology 21:825–828
Russo-Săndulescu D, Berza T (1979) Banatites from the western part of the southern Carpathians (Banat). Rev Roum Géol Géophys Géogr Géol 23(2):149–158
Russo-Săndulescu D, Berza T, Bratosin I, Ianc R (1978) Petrological study of the Bocşa banatitic massif (Banat). DS Inst Geol Geof 64:105–172
Russo-Săndulescu D, Vajdea E, Tanasescu A (1984) Neocretaceous-Palaeogene subduction igneous rocks in the romanian Carpathians – mutual relationships, succession and areal distribution. DS Inst Geol Geof 64:111–119
Russo-Săndulescu D, Bratosin I, Vlad C, Ianc R (1986a) Petrochemical study of the Surduc banatitic magmatites (Banat). DS Inst Geol Geof 70–71:97–121
Russo-Săndulescu D, Berza T, Bratosin I, Vlad C, Ianc R (1986b) Petrological study of banatites in the Ocna de Fier – Dognecea zone (Banat). DS Inst Geol Geof 70–71(1):123–142
Russo-Săndulescu D, Vajdea E, Tanasescu A (1986c) Significance of K-Ar radiometric ages obtained in the banatitic plutonic area of Banat. DS Inst Geol Geof 70–71:405–417
Săndulescu M (1994) Overview on Romanian geology. In: ALCAPA II Field Guideb South Carpathians and Apuseni Mountains. Rom J Tectonics Reg Geol 75(2): 3–15
Săndulescu M, Visarion M (2000) Crustal structure and evolution of the Carpathian-Western Black Sea areas. First Break 18(3):103–108
Savu H, Udrescu C, Lemne M, Romanescu O, Stoian M, Neacsu V (1987) Island-arc volcanics related to the wildflysch on the outer margin of the Danubian Autochton (southern Carpathians) and their geotectonic implications. Rev Roum Géol Géophys Géogr, Géol 31:19–27
Schmid SM, Berza T, Diaconescu V, Froitzheim N, Fügenschuh B (1998) Orogen-parallel extension in the southern Carpathians. Tectonophysics 297:209–228
Schmidt MW (1992) Amphibole composition in tonalites as a function of pressure : an experimental calibration of the Al-in-hornblende barometer. Contrib Mineral Petrol 110:304–310
Soroiu M, Catilina R, Strutinski C (1986) K-Ar ages on some igneous rocks from the south-western end of the South Carpathians (Banat Hills). Rev Roum Phys 31(8):849–854
Ştefan A, Roşu E, Andăr A, Robu L, Robu N, Bratosin I, Grabari G, Stoian M, Vâjdea E, Colios E (1992) Petrological and geochemical features of banatitic magmatites in northern Apuseni Mountains. Rom J Petrol 75:97–115
Ştefănescu M (1988) Geological cross-section at scale 1:200,000 across Romania, AB. Geological and Geophysical Institute, Bucharest
Steiger RH, Jäger E (1977) Subcommission on geochronology: convention on the use of decay constants in geo- and cosmochronology. Earth Planet Sci Lett 36:359–362
Strutinski C, Catilina R, Soroiu M, Todros C, Paica M (1986) Potassium-argon geochronology of the Alpine igneous activity within the south-western corner of the Poiana Ruscă massif (South Carpathians, Romania). Proc Geoinst Belgrade 19:107-121
Sun SS, McDonough WF (1989) Chemical and isotopic systematics of oceanic basalts: implications for mantle composition and processes. In: Saunders AD, Norry MJ (eds) Magmatism in ocean basins. Geol Soc Lond Spec Publ 42:313–345
Toplis MJ, Carroll MR (1996) Differentiation of ferro-basaltic magmas under conditions open and closed to oxygen: implications for the Skaergaard intrusion and other natural systems. J Petrol 37:837–858
Vander Auwera J, Longhi J, Duchesne J-C (1998a) A liquid line of descent of the Jotunite (Hypersthene Monzodiorite) Suite. J Petrol 39(3):439–468

Vander Auwera J, Bologne G, Roelandts I, Duchesne J-C (1998b) Inductively coupled plasma mass spectrometry (ICP-MS) analysis of silicate rocks and minerals. Geol Belg 1:1–10

Vassiliev L, Stanisheva-Vassilieva G (1981) Metallogeny of the Eurasian copper belt: sector Bulgaria. Geol Balcanica 11(2): 73–87

Vlad Ş-N (1974) Skarn mineralogy at Dognecea (in Romanian). Academiei, Bucharest

Vlad Ş-N (1979) A survey of banatitic (Laramian) metallogeny in the Banat region. Rev Roum Géol Géophys Géogr Géol 23(1):39-44

Vlad Ş-N (1997) Calcic skarns and transversal zoning in the Banat mountains, Romania : indicators of an Andean-type setting. Miner Deposita 32:446–471

Whalen JB, Currie KL, Chappell BW (1987) A-type granites: geochemical characteristics, discrimination and petrogenesis. Contrib Mineral Petrol 95:407–419

Willingshofer E (2000) Extension in collisional orogenic belts: the Late Cretaceous evolution of the Alps and Carpathians. PhD Thesis, Faculty of Earth Sciences, Vrije Universiteit Amsterdam

Wones DR (1989) Significance of the assemblage titanite + magnetite + quartz in granitic rocks. Am Mineral 74:744–749